THREE-DIMENSIONAL ANALYSES OF PRECAST CONCRETE FLOORING SYSTEMS USING FINITE ELEMENT MODELING OF SUBASSEMBLIES

by

Zachary P. Christopulos

A thesis submitted to the faculty of
The University of Utah
in partial fulfillment of the requirements for the degree of

Master of Science

Department of Civil and Environmental Engineering

The University of Utah

December 2014

The University of Utah Graduate School

STATEMENT OF THESIS APPROVAL

The thesis of **Zachary P. Christopulos**

has been approved by the following supervisory committee members:

Chris P. Pantelides	, Chair	**6-16-2014** Date Approved
Lawrence D. Reaveley	, Member	**6-16-2014** Date Approved
Luis Francisco Ibarra	, Member	**6-16-2014** Date Approved

and by **Michael Ernest Barber** , Chair/Dean of

the Department/College/School of **Civil and Environmental Engineering**

and by David B. Kieda, Dean of The Graduate School.

ABSTRACT

Precast concrete flooring systems are a fast and cost-competitive construction method. There are currently a number of precast products on the market, such as hollowcore decks, and double-T decks. Hollowcore decks and double-T decks have been on the market for a number of years. These systems have been shown to perform well under typical building loads. Recently, a number of other precast systems have been brought to the market. These systems include biaxial hollowcore decks, filigrees, and the Plattforms Flooring System. The newer systems have not had the same "proof testing" that the more seasoned precast systems have faced.

All new systems must be tested and analyzed prior to using them in a structure. Most tests performed on precast systems are uniform or symmetric loads placed on a single panel. Typical building loads are never uniform. Concentrated loads can occur in nearly every building type and at almost any location on the floor plate. These concentrated loads will typically create asymmetrical loadings on a given panel. The asymmetrical load on a single panel will affect the nearby panels. Typical uniform loading tests on a single panel do not quantify the effects of asymmetrical loads on a flooring system.

In order to analyze the effect an asymmetrical load has on a flooring system, a method has been developed of modeling a single panel connected to a simple substructure that mimics the stiffness of adjacent panels in the floor. By using this

substructure, the effect of loading a single panel with a concentrated load can be analyzed for an entire floor plate.

TABLE OF CONTENTS

ACKNOWLEDGMENTS

I would like to extend my gratitude to my graduate committee, Dr. Reaveley, Dr. Pantelides, and Dr. Ibarra. These men have pushed me to continuously try to improve this thesis, and turn it into a document that I can be proud of. I would also like to thank Daryl Hodgsen at Plattforms, Inc. for his guidance on the practical issues facing the Plattforms Flooring System. Finally, I would like to thank my wife for her love and support during this work. She has always been there to push me towards the finish line.

CHAPTER 1

INTRODUCTION

Precast concrete systems are not new to the construction industry. These systems afford the contractor an accelerated construction time, as well as plant-controlled quality assurance of the concrete product. Currently, the most common precast flooring systems are hollowcore decks, and double T-decks. Over the past several years, a number of other systems have been brought to the market. Some of the newer systems are filigrees, biaxial hollowcore systems, and Plattforms flooring system.

Currently, most precast flooring systems are designed assuming uniform loads. Individual panels are analyzed using the section properties of the system, the assumed uniform load, and the required span of the structure. In reality, loads are never uniform. A system behaves very differently depending on the location and magnitude of a load. Heavy line loads down the center of the longitudinal axis of a precast member creates deflections and stresses that are drastically different from a heavy line load at the edge of a panel. The loaded panel is not the only panel in the flooring system affected by the non-uniform load. Panels adjacent to the loaded panel have induced deflections that will create stresses in the panel and in the connections. For this document, the term "constructed condition" is used to describe a panel that is connected not only to a support system, but also to adjacent panels. Differentiating this term is important due to the fact that most tests and analyses of precast systems are performed on a single panel. These

single panel tests and analyses shed little light on the behavior of multiple panel systems. One cannot analyze asymmetrical loads on a constructed condition panel accurately with simple hand calculations. Fortunately, finite element analysis has become a commonplace tool in most structural engineering firms. Finite element programs such as ANSYS now allow for in depth three-dimensional analyses of structures. Although finite element analysis is very useful, there are several drawbacks to using three-dimensional analyses in flooring systems. The primary drawback is computing time. Even with high performance computers, a full three-dimensional model of a building built with three-dimensional elements is not feasible with typical computing capabilities. A single precast panel has hundreds of thousands of elements, which implies hundreds of thousands of equations that the computer must solve. Building a precast concrete model comprised of multiple panels and millions of elements is not feasible. An individual panel is, however, possible to analyze. In order to bridge the divide between analyzing a single panel and the constructed conditions of a precast flooring system, a method has been developed for analyzing a single panel that can represent the constructed conditions of an entire floor.

The purpose of this thesis is to show that one can model the constructed conditions of a precast flooring system by creating a three-dimensional finite element model of a single panel connected to a subassembly of simple one-dimensional elements that reflects the stiffness of the entire floor assembly. Once the finite element model of the panel and subassembly are created, any vertical loading condition can be analyzed.

The following document takes the reader through the development of the finite element modeling process described above. Although this method can be used on any precast flooring system, this document uses the Plattform flooring system to demonstrate the technique.

Chapter 2 gives a brief description of the Plattform system. Chapter 3 discusses various analytical methods that have been used to analyze the Plattforms system, as well as other precast systems. Chapter 4 describes the scope of this thesis. Chapter 5 examines the full-scale tests of the Plattform system that are used to compare to the analytical model. Chapter 6 shows verification testing of the elements that are used in the finite element model. Chapter 7 presents the single panel finite element model used to reflect the full-scale tests. Chapter 8 discusses a method for defining the constructed conditions subassembly. Chapter 9 shows how one can analyze asymmetrical loads on a floor with the constructed condition model. Chapter 10 discusses conclusions and further research on this method.

CHAPTER 2

A BRIEF HISTORY OF THE PLATTFORMS SYSTEM

Plattforms flooring system is a precast composite concrete and steel floor structure. This system differs from other composite systems in the manner in which composite action is developed. Steel wide flange members are connected to a concrete slab through a system of stem walls. These stem walls are not continuous along the length of the floor. The openings between the stem walls allow for mechanical and electrical equipment to run through the web of the system.

In April of 2008, the first prototype was developed. The original design was a double-T section with two steel joists connected to a 12 ft. wide concrete slab by a series of stem walls. Although the original design performed well structurally, Plattforms, Inc. found that a single-t section would be more efficient with material having a lower steel to concrete ratio.

The panel shown in Figure 2.1 is the current Plattform design. As can be seen in this figure, a steel beam is connected to the concrete slab by discontinuous concrete stem walls that allow for mechanical and electrical equipment to pass through. In order to help support the slab, four braces are connected at the edges of the slab and to the web of the steel section.

As the Plattform panel design evolved, so did the methods used to analyze the section. The original analytical model for the Plattform panel was a simple elastic beam

model. The tests showed that general elastic beam theory would not suffice in modeling this new flooring system. The elastic beam model assumed that all of the steel would be in tension like a typical composite section. Tests performed at the University of Utah showed that the steel was not entirely in tension, and that a portion of the steel went into compression (Burkhart, 2010). Other methods have been used to try to determine the mechanical properties of the system.

One method of analysis utilizes a strut-tie model to determine the capacity of the system, but this method is not currently used by Plattforms, Inc. (Burkhart, 2010). The current method of design used by Plattforms, Inc. utilizes a stiffness reduction factor that is based on the shear rigidity of the stem walls. This empirical method reflects the test data, and has become the dominant analytical model used to calculate the deflection of the various Plattforms configurations.

Although the current method of analysis used by Plattforms, Inc. correlates to the test data when uniform loads are applied, the shear reduction factor lacks substantial engineering rigor. The current model is also incapable of accurately analyzing asymmetrical load configurations or vibration effects. These types of loads could be created by heavy machinery, cars, or brick walls that are not in line with the steel beam in the longitudinal direction.

Figure 2.1: Current Plattform Panel

CHAPTER 3

PAST ANALYSIS OF THE PLATTFORMS SYSTEM

Small-scale testing of the Plattforms system was performed at the University of Utah (Burkhart, 2010). The panels tested had a 13 ft. span and 4 ft. wide slab. The depth of the members was 2 ft. 8 in. A single point load was applied to the center of the section. Several strain gages were used to determine the deformation of the system under loading. These tests showed the first cracking failures to occur in the exterior stem walls with approximate 45 degree cracks first appearing at the head location of the nelson studs. The strain gages that were connected to the steel section showed that the neutral axis of the section actually lied in the steel beam at 7.5 in. above the bottom flange. The steel member used in these tests was a W10×12, which implied that much of the steel section was in tension (Burkhart, 2010).

The original analysis of the Plattform panels utilized conventional Euler-Bernoulli beam theory to analyze the capacity of the sections. Using this method, it was assumed that shear is transferred linearly from tension in the steel section to compression in the concrete slab. However, Burkhart (2010) performed experimental tests on Plattform panels, showing that the strain distribution as a function of height at yield and ultimate failure loads is not linear, and that compression occurs in the top of the steel beam.

During the analysis phase, Burkhart created a strut tie model of the Plattforms system. Although the model was not able to analyze the capacity of the system directly,

the strut tie model did shed some light on the load path of the system. Through the analysis, it was found that without substantial changes to the locations of the stem walls, there will always be some compression in the steel flange. Brett explained that compression in the steel flange is due to the compression struts in the steel web landing below an opening in the stem walls. The openings do not allow for the compression strut to continue up to the concrete slab. To satisfy equilibrium, the compression strut must then place compression into the flange of the steel beam (Burkhart, 2010).

To account for the difference in stiffness between the Euler-Bernoulli model and test data, Plattforms, Inc. uses a stiffness reducing factor that is based on the shear rigidity of the concrete shear walls. Although there is not a substantial amount of analytical support behind the stiffness reducing factor, the deflection results of the analysis do show good correlation with test data. Currently, Plattforms Inc. uses the stiffness reducing factor in their analytical model for panel design.

Up to this point, all of the research on the Plattforms system has been either uniform, or symmetrical. None of this analysis can shed much light on the effects of asymmetrical loads. Other researchers have made attempts at analyzing the effects of asymmetrical loads on precast flooring systems. For instance, Stanton (1992) utilizes two computer models to analyze these effects. The first model is a uniform plate analysis that ignores the joints between the hollow-core panels. The second model is a strip method that uses different elements to analyze the joints between the panels. Stanton assumes the joints in the second method to behave as “piano hinges” that do not transfer transverse moments. The purpose of Stanton’s study is to define design rules that would allow structural engineers to distribute concentrated loads to adjacent panels to allow for less conservative design. Although this method provides guidance on the qualitative two-way

bending behavior of a hollow-core floor, it is not capable of analyzing directly the stresses induced at connection locations.

Chen (1999) uses a similar qualitative procedure for analyzing the transfer of loads across panels. Chen analyzes double-T sections as a slab comprised of four node shell elements sitting on top of stems comprised of linear two node beam elements and considers the joints as hinges that cannot transfer transverse moments.

The methods presented by Stanton and Chen provide qualitative analysis of a constructed condition flooring system where panels are connected through continuous "piano hinge" elements. They cannot, however, show in depth stress distributions in a panel, nor are they capable of analyzing the stresses at connection points that are typically discrete. The method presented in this thesis is capable of modeling both the constructed conditions of a panel, as well as showing accurate stress contours of a panel under concentrated asymmetrical loads.

Figure 3.1: Failure of Small-Scale Panel (Burkhart, 2010)

CHAPTER 4

SCOPE OF RESEARCH

Although the analysis of the Plattforms system has progressed, there are still a number of questions that cannot be answered by any of the analytical techniques that have been utilized. Performance of the system under asymmetrical loads, vibration performance, and capacity of the system with mechanical holes punched in the slab cannot be not analyzed with current methods. To address some of these items, a methodology has been developed that can model the constructed condition performance of the Plattforms system through a subassembly of linear elements created in the finite element software ANSYS. This study shows that one can use a finite element software program, and the method developed in this document, to analyze the constructed condition performance of the system. The method used to model and analyze the performance is as follows:

1. Perform verification testing of elements that will be used in the finite element model to ensure understanding of the constitutive relationships used by the software;
2. Create a finite element model of a single panel;
3. Compare the results of the finite element model to test results;
4. Modify the model to reflect the constructed conditions by varying the boundary conditions;

5. Create floor plan loading scenarios for the structure to represent a wide range of possible conditions;
6. Apply appropriate loads to the finite element model (these could include vibratory loads); and
7. Interpret results and modify design if necessary.

CHAPTER 5

MOUNTAIN STATES STEEL TEST

The panels tested during the full-scale tests at Mountain States Steel had a 45 ft. span and a 3.5 ft. depth. Incrementally increasing uniform loads were placed on the panels, and the deflections at each increment were recorded. The following chapter describes the tests performed at Mountain States Steel. Section 5.1 describes the testing set up. Section 5.2 shows the panel-to-girder connections of the test. Section 5.3 displays the results of the test.

5.1 Test Setup

Figure 5.1 shows the plan view of the test. Three precast panels were tested. Panels 1-3 rested on girder1 and girder2. Each of the panels had slight changes in geometry. Panel 1 was the conventional Plattform panel, and was the panel modeled for this document. Deflection sensors were placed at the girder connection location of each panel and at the midspan to calculate the maximum relative deflection of the panel.

Figure 5.2a shows the elevation side view of panel 1. Figure 5.2b shows the elevation view of girder2. The girder has a similar design to the panels. As can be seen in Figure 5.2b, the girder is made up of a steel beam, with a composite concrete wall cast on top of it. The uniform loads applied to the panels were created by placing 45 ft. × 8 ft. × 1 in. steel plates across each panel. Each plate applied a pressure to the system of about

40 psf.

Details of the geometric configuration for panel 1 can be seen in Figure 5.3. This figure is the shop drawing used by Mountain States Steel to manufacture the test panels. As can be seen in Figure 5.3, the 45 ft. × 8 ft. × 3 in. slab is reinforced with #4 bars spaced at approximately 9 in. on center down the center of the slab, as well as welded wire fabric that has roughly the same dimensions as the slab. The slab rests on nine concrete stem walls that are 2 ft. 2-¾ in. tall. The seven interior stem walls are 2 ft. long, while the two exterior stem walls are 4 ft. 10 in. long. The reason the exterior stem walls are longer is due to previous testing showing that the exterior stem walls are the first places to fail. Failure at the exterior stem wall is due to the large shear stresses that develop at the reaction locations. The stem walls are reinforced with vertical DBAs (deformed bar anchors) spaced at 12 in. on center with a 90 degree bend into the slab (see panel a in Figure 5.3); additionally, there is horizontal reinforcing at 8 in. on center. The stem walls are connected to the beam with ¾ in. × 6 in. nelson studs spaced at 6 in. on center for the exterior stem walls and at 9 in. on center for the interior stem walls. Angle braces extend from the slab to each side of the web of the steel beam at approximately 9 ft. on center.

5.2 Panel-to-Girder Connections

The Plattform panels were connected to the girders in two ways: a saddle connection that held the steel beam, and a slab connection created by welding plates across embeds in the under-side of the slab and the concrete web of the girder. Figure 5.4a shows the saddle connection. The saddle is welded to the steel web of the girder beam. Approximately 6 in. of the W12×22 Plattform panel beam sits in the saddle. Once

the panel is placed in the girder saddle, the flanges of the steel beam are bolted to the base of the saddle.

The slab-to-girder connection can be seen in Figure 5.4b. This figure shows the welded plate over the slab and girder embeds.

5.3 Results of the Mountain States Steel Tests

The deflection of the panel was measured from the center of the steel beam. The recorded deflection values were taken after the deflection from self-weight had already taken place. Figure 5.5 shows the center line deflection values of the panel at various loads.

As Figure 5.5 demonstrates, the slope of the deflection curve remained fairly constant until about a 120 psf load was reached. The change in slope beyond this point indicates that in order to accurately model the deflection of the Plattform panel above a 120 psf load, a nonlinear model should be used.

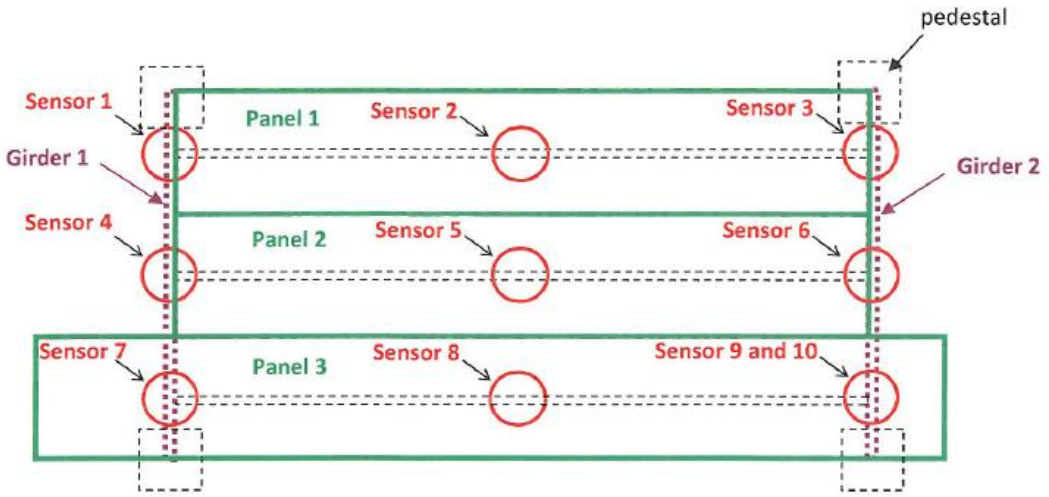

Figure 5.1: Plan View of Tests (Western Technologies 2010)

a b

Figure 5.2 Panel and Girder Elevations. a) Elevation of Panel b) Elevation of Girder

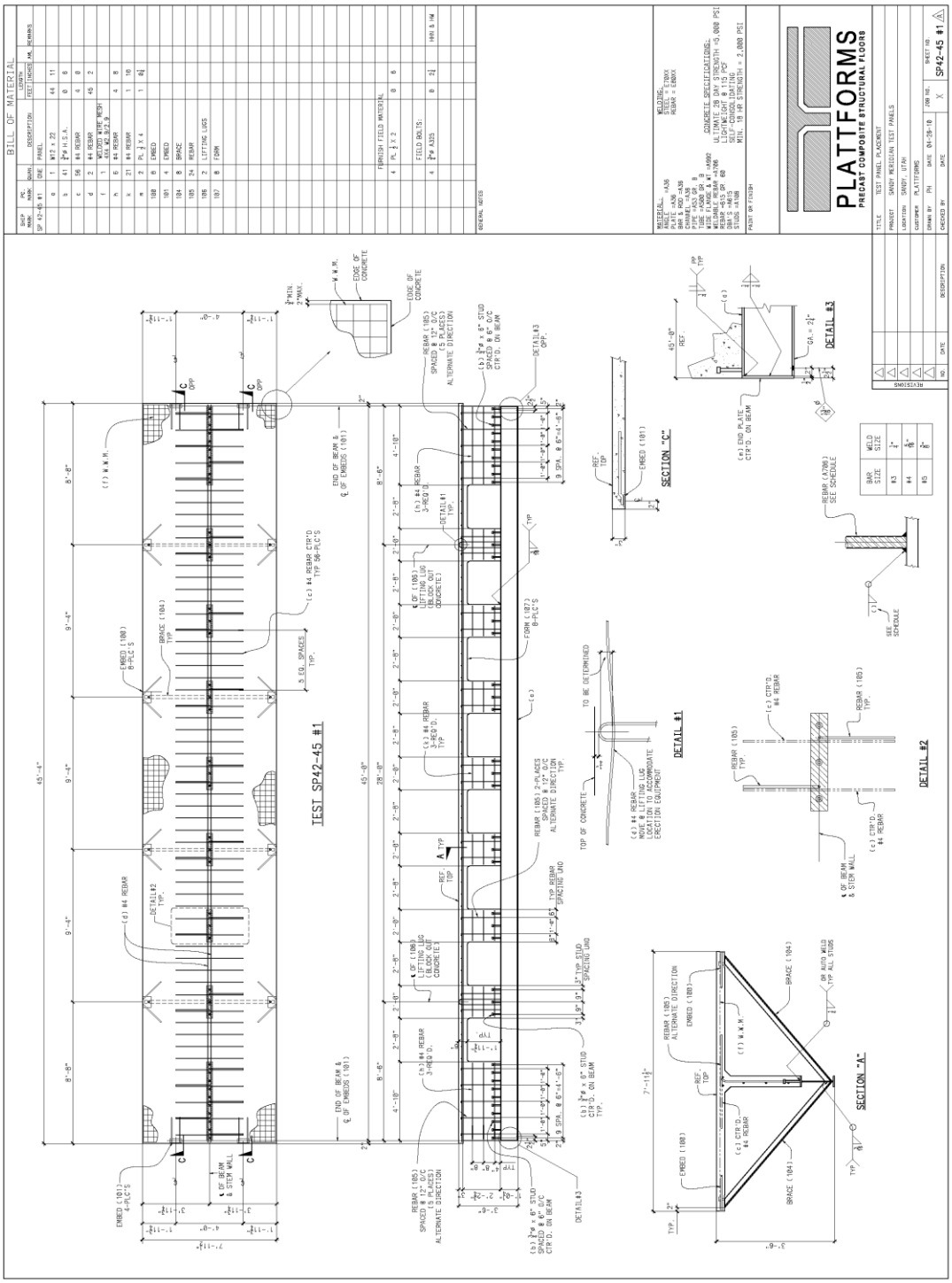

Figure 5.3: Panel Shop Drawings

a b

Figure 5.4 Panel Connections a) Saddle Connection b) Slab-to-Girder Connection (Western Technologies, 2010)

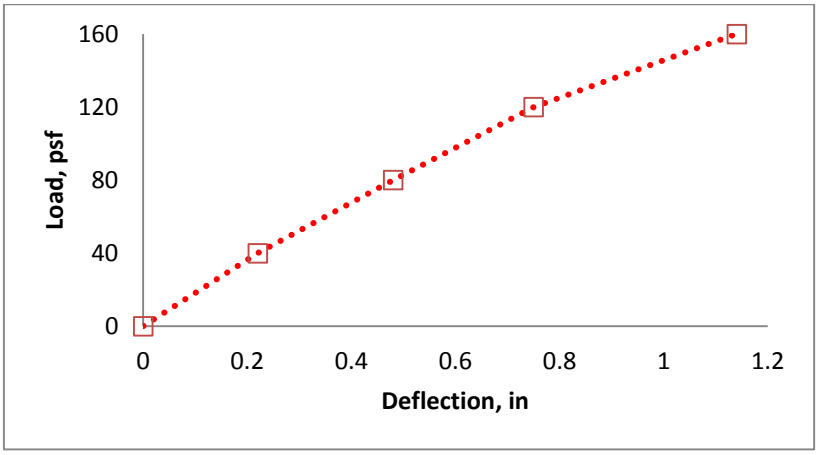

Figure 5.5: Mountain States Steel Test Results (Western Technologies, 2010)

CHAPTER 6

ELEMENT VERIFICATION

Chapter 6 presents simple verification testing of the elements used in the model. The following ANSYS elements were used to create the original finite element model: Solid45, Solid65, and Link8. From these elements, only the Solid65 element is nonlinear. Section 6.1 discusses the mechanics properties of the Solid45 element. Section 6.2 discusses the mechanics properties of the Link8 element. Section 6.3 discusses the mechanics properties of the Solid65 element.

6.1 Solid45 Element

The Solid45 element is an 8 node hexahedral linear element. This element is based on the three-dimensional mechanics relationship presented in Equation 6.1, where D is a 6×6 matrix, and both σ and ε are 6×1 vectors.

$$\boldsymbol{\sigma} = \mathbf{D} \cdot \boldsymbol{\varepsilon} \tag{6.1}$$

Equation 6.2 shows Equation 6.1 in explicit form. The 6×1 vector σ defines the axial and shear stresses in an element corresponding to the axial and shear strains of the 6×1 vector ε. Note that the matrix D shown in 6.2 assumes an isotropic material with constant Young's Modulus (E), Poisson's Ratio (v), and Modulus of Rigidity (G). Although this

project assumes all materials are isotropic, the Solid45 element can be used to model anisotropic materials with different E, v, and G in the x, y, and z directions.

$$\begin{bmatrix} \sigma_x \\ \sigma_y \\ \sigma_z \\ \tau_{xy} \\ \tau_{xz} \\ \tau_{yz} \end{bmatrix} = \begin{bmatrix} \frac{(v-1)E}{v-1+2v^2} & -\frac{vE}{v-1+2v^2} & -\frac{vE}{v-1+2v^2} & 0 & 0 & 0 \\ -\frac{vE}{v-1+2v^2} & \frac{(v-1)E}{v-1+2v^2} & -\frac{vE}{v-1+2v^2} & 0 & 0 & 0 \\ -\frac{vE}{v-1+2v^2} & -\frac{vE}{v-1+2v^2} & \frac{(v-1)E}{v-1+2v^2} & 0 & 0 & 0 \\ 0 & 0 & 0 & G & 0 & 0 \\ 0 & 0 & 0 & 0 & G & 0 \\ 0 & 0 & 0 & 0 & 0 & G \end{bmatrix} \cdot \begin{bmatrix} \varepsilon_x \\ \varepsilon_y \\ \varepsilon_z \\ \gamma_{xy} \\ \gamma_{xz} \\ \gamma_{yz} \end{bmatrix} \quad (6.2)$$

One of the simplest ways to understand the behavior of an element is through single element analysis. Single element analysis is the act of putting an element through various loads or deformation states, and then comparing those results to hand-calculated answers based on the constitutive model of the element.

The next examples use the following material properties: E = 2.88 e6 psi, v=0.2, G = 1.2 e6 psi. If one places a uniform load of 8 lbs. in the y direction (y being the vertical direction) on an element of dimensions 1×1×1 in.^{3}, and restricts strain in all directions except in the direction of the load, one could find the strain in the y direction by a hand calculation. Because the strain is zero in all directions except the y direction, Equation 6.2 simplifies to:

$$\sigma_y = \frac{(v-1)E}{v-1+2v^2}\varepsilon_y \quad (6.3)$$

Solving for ε_y yields Equation 6.4.

$$\varepsilon_y = \frac{\sigma_y}{\frac{(v-1)E}{v-1+2v^2}} = \frac{8}{3.2E6} = 0.25\ e-5 \tag{6.4}$$

Because the element has a length of 1 in., the strain is equal to the deflection.

When the correct commands are applied to ANSYS, the loading condition defined in Equation 6.4 can be created. The results from ANSYS are presented in Figure 6.1. The maximum deflection value on the contour legend is the same value found from Equation 6.4. One should note that 0.25 e-5 in. is not the value found from the one-dimensional Hooke's Law. If one-dimensional Hooke's Law is used, Equation 6.5 is found.

$$\sigma = E\varepsilon = 8 = 2.88\ e6 \cdot \varepsilon \tag{6.5}$$

Equation 6.5 implies that the strain is actually 0.278 e-5, as shown in Equation 6.6.

$$\varepsilon = \frac{\sigma}{E} = \frac{8}{2.88\ E6} = 0.278\ e-5 \tag{6.6}$$

The difference in strain is due to the fact that the single element test presented in Equation 6.4 is a uniaxial strain model. Hooke's Law is a uniaxial stress model. Note that Hooke's Law gives a strain that is greater than the strain calculated by ANSYS. The ANSYS model is stiffer because it includes Poisson's effect. Because no strain is allowed in any direction other than the y direction, a multiaxial stress state is created.

Although the one-dimensional Hooke's Law does not apply to the single element

test, the Solid45 element is capable of modeling a one-dimensional shape under uniaxial stress. If one creates a long rectangular rod with dimensions $1 \times 100 \times 1$ in.^{3} comprised of 100 Solid45 elements with a stress of 8 psi pointing in the y direction, the strain in the rod can be found in Figure 6.2. Note that the displacement in Figure 6.2 is 0.278e-3 in. The strain in the rod can be found by Equation 6.7.

$$\varepsilon = \frac{\Delta L}{L} = \frac{0.278\ e-3}{100} = 0.278\ e-5 \tag{6.7}$$

The results from Figure 6.2 and Equation 6.7 show that the Solid45 element can model the one-dimensional Hooke's Law in Equation 6.6.

A single element test can also be performed for shear strain. Suppose one applies a load along the top of the cube in the x direction (x being the horizontal direction) holding the top plane of the cube from displacing in the y direction (y being the vertical direction). From Equation 6.2, the shear state of a single element can be found by:

$$\tau_{yx} = G\gamma_{yx} = 8 = 1.2\ e6 \cdot \gamma_{yx} \tag{6.8}$$

Solving for the shear strain gives Equation 6.9.

$$\gamma_{yx} = \frac{\tau_{yx}}{G} = \frac{8}{1.2\ e6} = 0.667\ e-5 \tag{6.9}$$

Analyzing the shear loading condition in ANSYS gives the deflection results presented in Figure 6.3. Figure 6.3 shows that the maximum displacement is 0.667 E-5. The strain γ can be found by Equations 6.10 and 6.11.

$$\tan(\gamma) = \frac{\Delta}{L} = \frac{0.667\ e-5}{1} = 0.667\ e-5 \tag{6.10}$$

Because γ is small:

$$\tan(\gamma) \approx \gamma = \frac{\Delta}{L} = 0.667\ e-5 \tag{6.11}$$

As shown in the previous examples, the constitutive model for the Solid45 element is understood for the plane strain, the plane stress, and simple shear loading case. However, this project primarily focuses on the beam properties of the Plattform flooring system. If given a long slender section with the same dimensions as the section described in the uniaxial stress example, one can apply a load transverse to the longitudinal axis to verify that the Solid45 element can be used to analyze beam properties. Suppose an 8 lb. load is applied in the x-direction of the rectangular rod at one end, and held fixed at the other. The analytical solution to deflection is given by Equation 6.12.

$$\delta = \frac{PL^3}{3EI} = \frac{8 \cdot 100}{3 \cdot 2.88\ e6 \cdot \frac{1}{12}} = 11.119\ \text{in.} \tag{6.12}$$

Figure 6.4 shows the results found by ANSYS using the Solid45 element. As shown in this figure, the results are nearly identical to the Euler-Bernoulli solution.

6.2 Link8 Element

The Link8 element is a uniaxial stress element, and is commonly used to model trusses, cables, and springs. Each Link8 element has two nodes with three degrees of freedom per node. This element is used to model the braces, springs, and rebar in this project. To understand how the Link8 element works, one only needs to understand Hooke's Law. This elementary mechanics rule was presented in Equation 6.5. A steel bar that has a 1 in.^{2} area and 1 in. length, stretched by a force of 2 lbs., has a change in length equal to the value given in Equation 6.13.

$$\varepsilon = \frac{\sigma}{E} = \frac{2}{29E6} = 0.69\ e-7 \tag{6.13}$$

(The change in length equals the strain because the original length is 1 inch). Figure 6.5 shows the ANSYS output of this loading condition for a single Link8 element.

6.3 Solid65 Element

The Solid65 element is an 8 node hexahedral nonlinear element that is based on the Solid45 element. In the elastic range, the Solid65 element behaves identically to the Solid45 element. The nonlinear behavior is modeled based on the Willam-Warnke yield criterion (ANSYS Elements Reference, 2005). The Willam-Warnke failure surface is determined according to five input strength parameters. For this project, the only parameters used were the cracking capacity, and crushing strength of concrete. Using only the cracking and crushing capabilities of the Solid65 element, the element cracks if the first principal stress reaches a critical value. Similarly, the element crushes when the third principal stress reaches a critical value.

Once the element has cracked along the principal stress direction, the element loses stiffness in the direction perpendicular to the crack plane. In order for the element to maintain some stiffness, rebar can be placed in the element. If rebar is not present and the element cracks losing all stiffness in the perpendicular direction, deflections will be infinite, and the simulation will fail to converge. The rebar can be placed either as a "smeared" steel, or as Link8 elements. The following single element example demonstrates how the rebar works using a Link8 element.

Suppose a 1×1×1 in.^{3} Solid65 element has a simple tensile load of 8 lb. in the y direction. The maximum first principal stress is input as 0 psi. The element has four Link8 elements along the vertical edges of the Solid65 element. Each Link8 element has an area of 0.01 in., and a modulus of elasticity of 29 e6 psi. If the Solid65 element has zero tensile capacity, only the Link8 elements take the load, and the element strains according to Hooke's Law as shown in Equation 6.14. Figure 6.6 shows the strain calculated by ANSYS is identical to the strain from Equation 6.14.

$$\varepsilon = \frac{\sigma}{E} = \frac{\frac{8}{4 \cdot 0.01}}{29000000} = 0.69\ \text{e} - 5 \tag{6.14}$$

The same result can be found if the third principal stress reaches a critical value. The element crushes, and loses stiffness along the third principal stress plane. Figure 6.7 shows the same element from Figure 6.6 with a compressive force of eight lbs. on the element. Note that the maximum displacement is the same as that in Figure 6.6 in absolute value.

The previous examples show that once the first and third principal stresses of the

Solid65 element have reached a critical value, the element loses all stiffness in the direction perpendicular to the first and third principal stress plane.

Note that the preceding examples are for a plane strain condition. Most of the elements in the model for this research undergo various loading conditions other than simple plane strain. Pure shear can also create a first principal stress that is greater than the ultimate tensile capacity of the element. In this case, the shear transferred over the first principal plane is adjusted using shear transfer coefficients. The shear transfer coefficients reduce the shear stiffness of the element by a factor between 0 and 1. Two shear transfer coefficients are used for the Solid65 element, an open crack shear transfer coefficient, and a closed crack shear transfer coefficient. The open crack shear transfer coefficient is considered to be less than the closed crack shear transfer coefficient.

More advanced nonlinear models utilize size effects in order to predict failure. Concrete does not always fail at the prescribed tensile load for every test. The variability in load tests is due to inherent discontinuities in the concrete structure. A greater number of these discontinuities are found in larger samples. The greater number of discontinuities implies that larger concrete samples fail at lower stresses. Models can be created that reflect the probability of discontinuities, and are very important when analyzing a hydrostatic stress case, and one wants to find the crack pattern. Probabilistic models are not as important when analyzing the capacity of the Plattform system due to the fact that cracking consistently occurs in a known location. The goal of the model is not to predict cracking, but to model the effect of the reduced strength due to cracking.

Another reason size effects are not as critical for the Plattforms flooring system is that the dimensions of the stem walls are not significantly different from the typical concrete test cylinders used to determine the compressive strength of the concrete

sample. Typical concrete test cylinders are between 4 in. to 6 in. in diameter. The concrete stem walls in this project are 4 in. thick. Due to the fact that the stem walls and the typical test cylinders have comparable dimensions, size effects are ignored for this project.

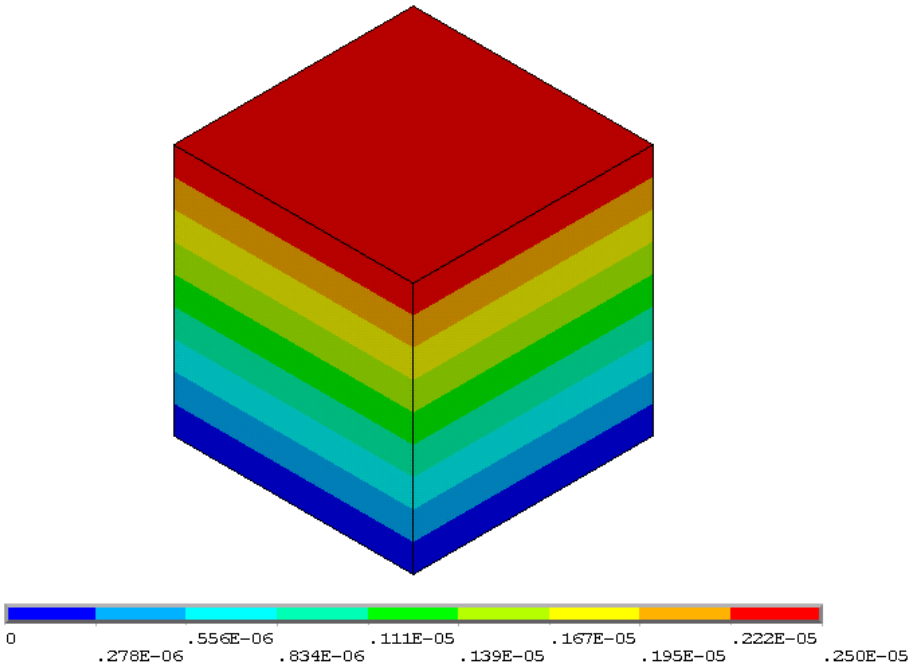

Figure 6.1: Solid45 Single Element Tension Test

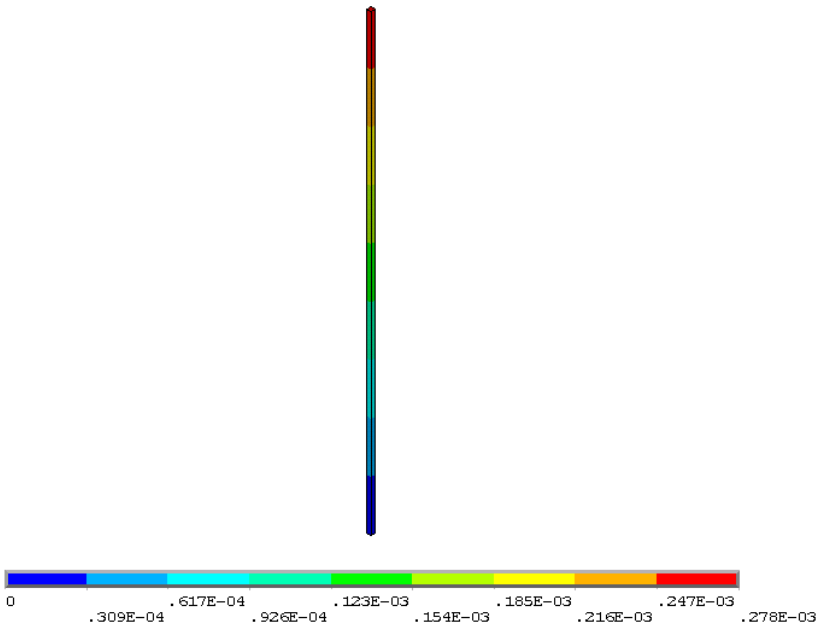

Figure 6.2: Solid45 Multiple Element Uniaxial Tension Test

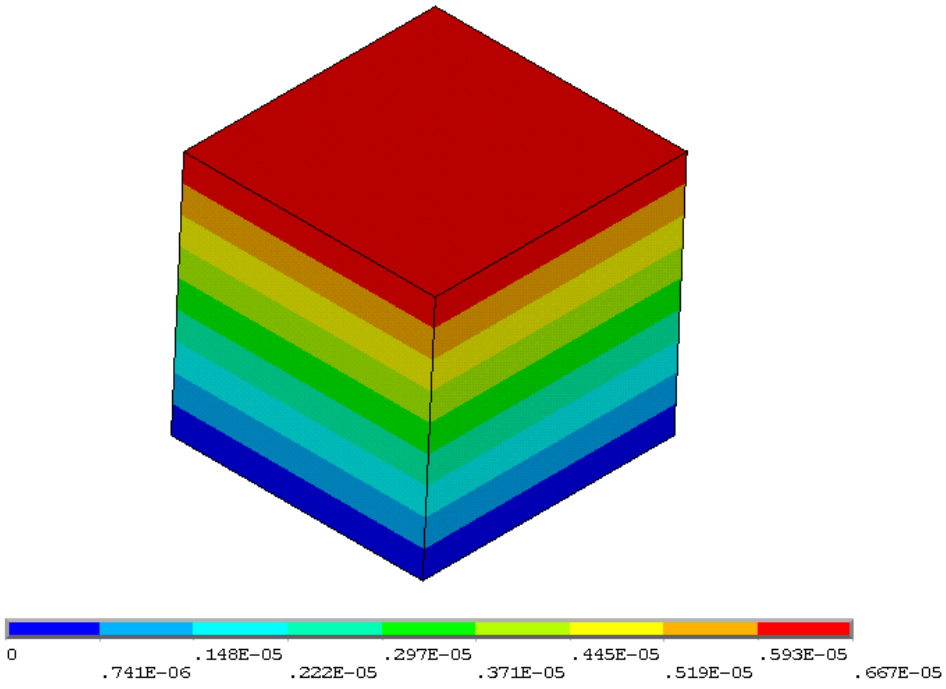

Figure 6.3: Solid45 Singe Element Shear Test

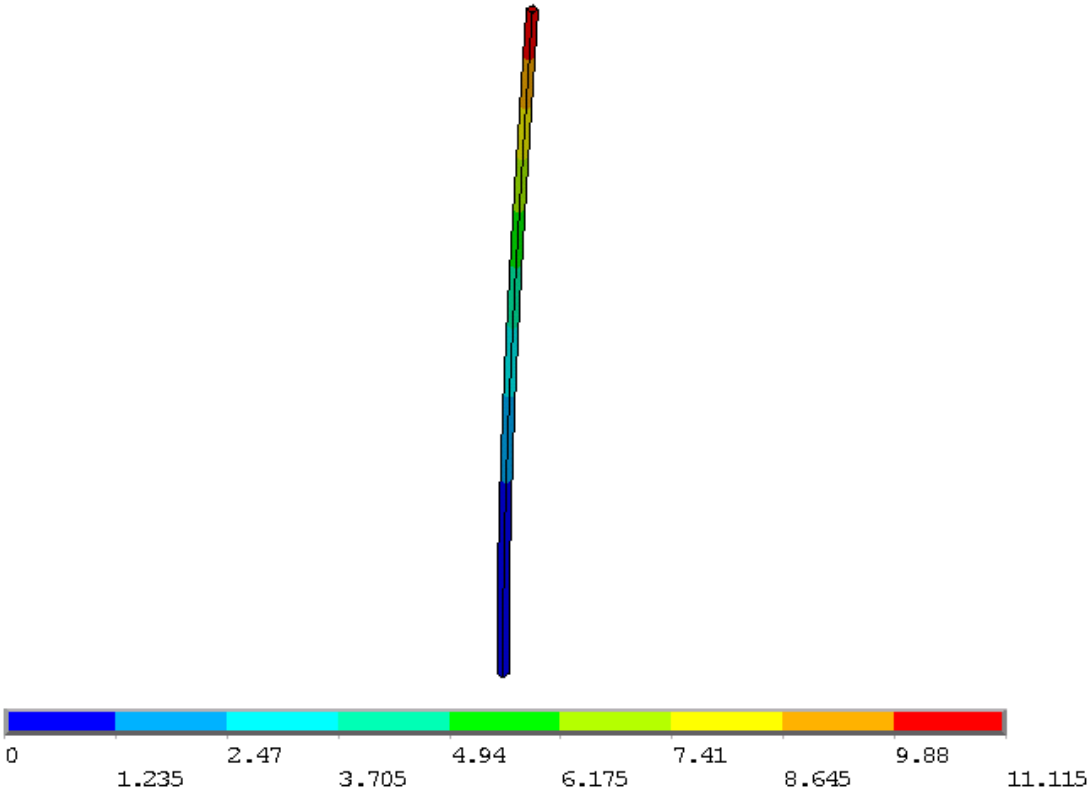

Figure 6.4: Solid45 Bending Properties

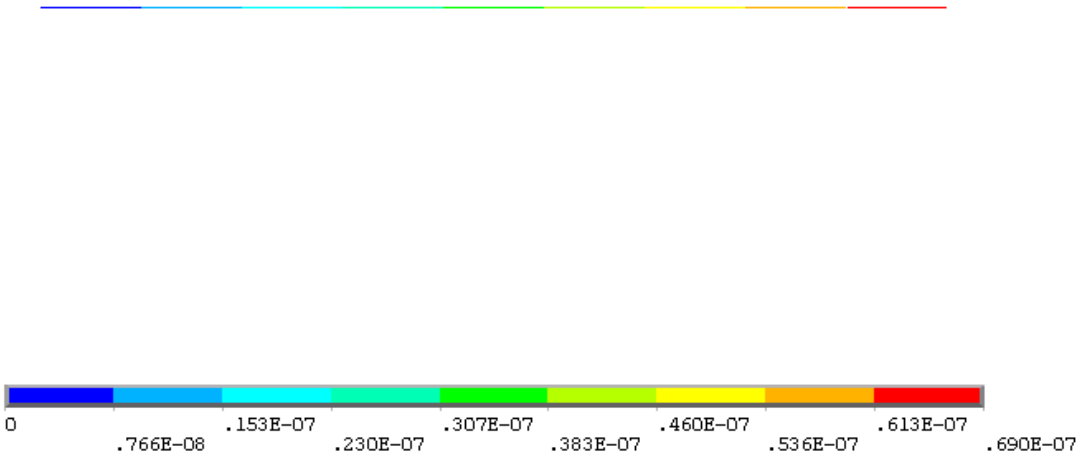

Figure 6.5: Link8 Element Axial Strain

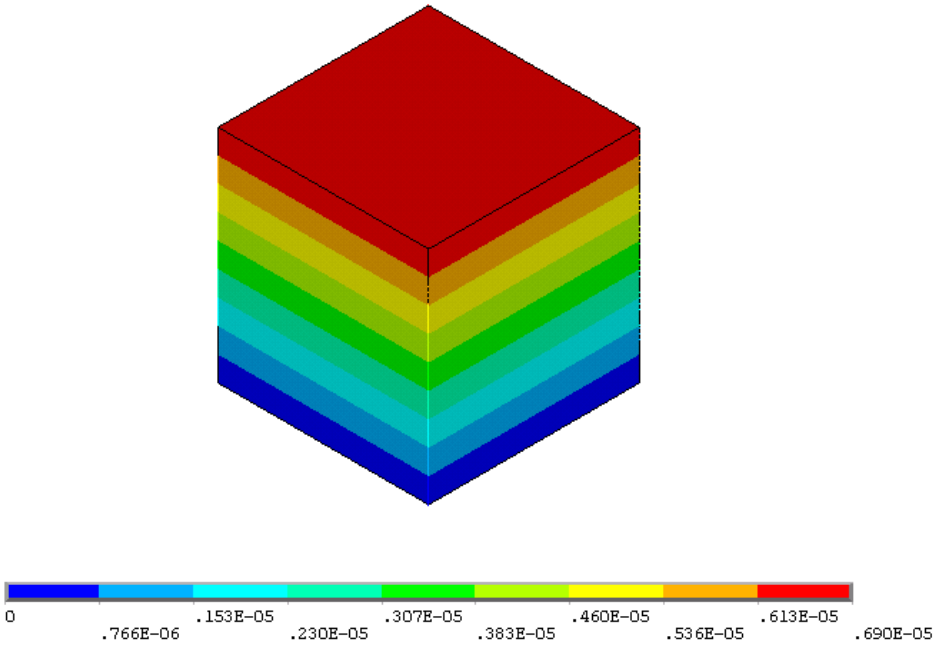

Figure 6.6: Solid65 Single Element Tension Test

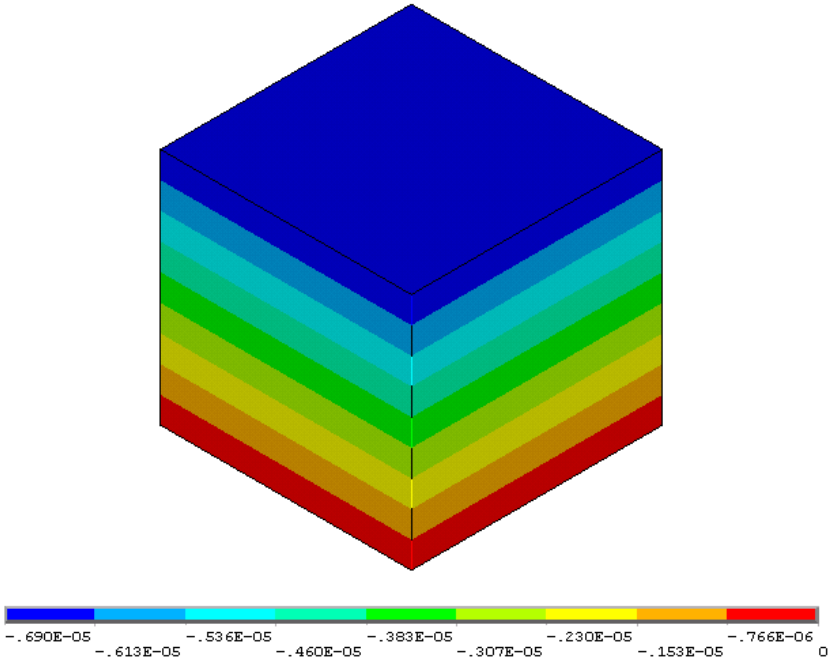

Figure 6.7: Solid65 Single Element Compression Test

CHAPTER 7

FINITE ELEMENT MODEL

This chapter addresses the various aspects of the finite element model created to predict the test performed at Mountain States Steel. Section 7.1 shows that due to symmetry, a ¼ panel section can be used for the analysis. Section 7.2 describes the finite element layout of the model. Section 7.3 outlines the material properties of the model. Section 7.4 displays three boundary conditions and the results of the model utilizing these boundary conditions.

7.1 Symmetry of the Finite Element Model

Symmetric models reduce computing time, and do not affect the results of the model for symmetric loading conditions. A symmetric model can be created by enforcing the appropriate boundary conditions on the planes through which the section is "cut". Figure 7.1 illustrates the symmetric Plattform model and the full-scale Plattform model.

The midspan of a simply supported beam has zero rotation under a uniform load. Rotation in a beam implies that a section cut through the beam that was once vertical in the unloaded state becomes angled after the beam is loaded. The angle the section cut makes from the vertical is due to material displacing in the longitudinal direction of the beam about the section cut. Zero rotation of a beam implies that the vertical section cut through the beam at the location of zero rotation remains vertical after the beam is

loaded. A vertical section cut after the beam is loaded implies that material does not displace in the longitudinal direction of the beam at the section cut. A simply supported, uniformly loaded beam has zero rotation at the midspan. From a finite element modeling perspective, the full-scale model can be cut in half at midspan by forcing the nodes at the midspan to have zero displacement in the longitudinal direction of the beam.

The three-dimensionality of the Plattform panel implies that the structure can bend in the transverse direction, as well as the longitudinal direction. The same logic used in the previous paragraph can be applied in the transverse direction. Figure 7.2 shows the transverse bending of a full panel under a uniform load. The slab in Figure 7.2 has zero rotation at the center; therefore, the model can be cut in half down the center with the center nodes prevented from translating in the transverse direction.

To ensure that the symmetric assumption is valid, both a symmetric and full size analyses were executed with the same loading condition. The deflection of the two different models are highlighted in Figures 7.3a and b, which shows that the symmetric model can be used to model the uniform load without loss in accuracy.

7.2 Element Layout

Solid45, Solid65, and Link8 elements make up the finite element model for this project. The Solid65 element is the only nonlinear element. The tests performed on the Plattform Flooring System show that the stem walls are the primary location of cracking. Plane sections only remain plane if the stem walls are infinitely rigid, and no shear deformation can take place. The stem walls are not rigid, and they do sustain deformation as they try to transfer the tension stress in the steel beam to the concrete slab as a compression stress. The shear placed on the stem walls creates a maximum first principal

stress at 45 degree angles near the saddle connections. Figure 7.4 shows the cracking of the stem walls under 200 psf load.

As the stem walls crack, they lose stiffness and the system's performance becomes nonlinear. To save on computation time, only the elements in the stem walls are modeled using the Solid65 elements. By only making the stem wall elements nonlinear, the model runs more efficiently, without a substantial loss in accuracy.

The concrete slab and the steel beam are assumed to behave linearly. These sections are modeled with Solid45 elements. The braces and rebar are modeled using Link8 elements. Figure 7.5a shows the solid elements of the ¼ finite element model. Figure 7.5b shows the line elements used in the ¼ finite element model.

7.3 Material Properties

The material properties used in the model are based on those measured in the Mountain States Steel tests. Table 7.1 displays the material properties of the steel and concrete that are used for the finite element model.

Note that the yield strength of the steel is not included in the table due to the fact that the steel is assumed to behave elastically. The modulus of elasticity of concrete is computed using the ACI formula (ACI 318, 2008):

$$E_c = 33 \cdot w_c^{1.5} \cdot f'c^{0.5} \tag{7.1}$$

where:

w_c= weight of concrete in $\frac{\text{lb.}}{\text{ft.}^3}$

f'c= 28 day compressive strength of concrete in psi

The cracking stress of concrete is calculated using the ACI formula (ACI 318, 2008):

$$\text{Cracking Stress} = 7.5\text{f}'\text{c}^{0.5} \tag{7.2}$$

The Solid45 elements are linear, and only require as input the modulus of elasticity, density, Poisson's ratio, and the shear modulus. Solid65 elements require shear transfer coefficients that can be used to change the element's nonlinear behavior. In Strengthening of Concrete Having Shear Zone Openings Using Orthotropic CFRP Modeling, Ashraf Mohamed Mahmoud uses shear transfer coefficients of 0.3 for open cracks, and 0.5 for closed cracks. These same shear transfer coefficients are also used in the work of Hawileh, et al. in Nonlinear Finite Element Analysis and Modeling of Precast Hybrid Beam-Column Connection Subjected to Cyclic Loads. The shear transfer coefficients used for this thesis are 0.2 for open cracks, and 0.5 for closed cracks. These values maintain numerical stability, as well as help the model match the test data (Hawileh, et al., 2010; Mahmoud, 2012).

7.4 Boundary Conditions and Model Results

Three different boundary conditions are analyzed: a pinned-pinned connection, a pinned-roller connection, and a pinned-roller with spring connection. A pinned-pinned connection for a three-dimensional finite element model implies that the nodes that sit inside the saddle connection do not translate in any direction. Figure 7.6 shows that the pinned-pinned boundary condition gives results that are too stiff.

The pinned-pinned boundary condition prevents the nodes in the saddle connection from displacing in the longitudinal direction. Releasing restraint in the

longitudinal direction creates a pinned-roller connection. Figure 7.7 depicts the results of the simulations with the pinned-roller boundary conditions. This model gives better results, but the deflections are slightly larger than that of the test data.

Structural components do not behave as pinned-pinned, or pinned-roller connections. In the Mountain States Steel tests, the girder provides torsional stiffness. One can model the stiffness of the girder by building a linear finite element model of the girder section. A linear model is reasonable to assume due to the fact that the girder did not show any cracking with a load of 160 psf. Under the assumption that the three panels apply roughly the same reaction forces to the girder, one can find the torsional stiffness of the girder by applying a horizontal load to the top of the girder at the slab connection locations, and finding the displacements at the connection points. Similarly, one can place horizontal loads at the saddle locations, and the deflections at these points can be found.

Figure 7.8 shows the deflection of the entire girder with a 200 lb. horizontal load at the saddle locations. The saddle load is applied at the midspan of the girder at the bottom of the steel beam section. Figure 7.9 illustrates the deflection of the girder with 100 lb. horizontal loads at each of the two slab connections (200 lbs. total). The two slab loads are applied 2 ft. off of each side of the midspan of the girder at the top of the concrete stem walls.

The torsional stiffness provided by the girder connection is modeled using the Link8 elements with stiffness based on the panel deflections shown in Figure 7.8 and 7.9. Figure 7.10 shows the results of the pinned-roller with spring connections. As Figure 7.10 reflects, the pinned-roller with spring connections matches test data very closely.

The preceding section shows that using the appropriate boundary conditions, and

the material parameters from section 7.3, the finite element model closely reflects test data. The actual boundary conditions the Plattform panel sees in its final constructed state are substantially different than the testing boundary conditions. Although the boundary conditions may change, the preceding section has shown that the material parameters and element layout for the finite element model have been validated against one full-scale load test.

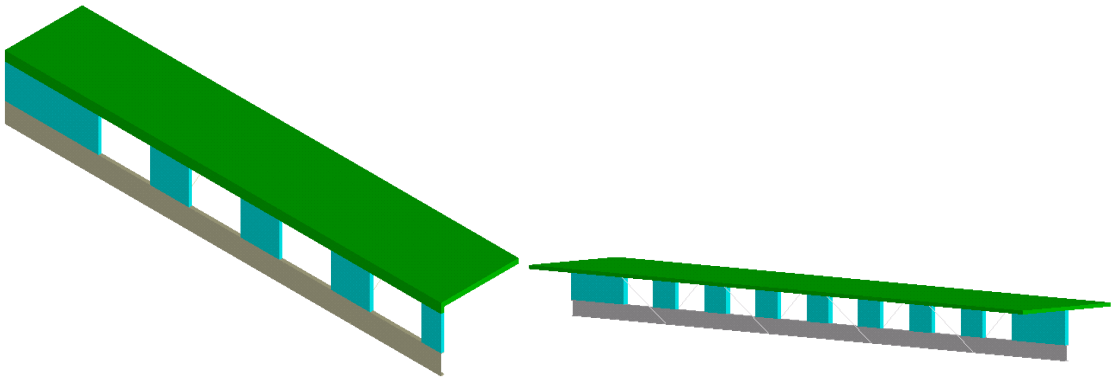

a b

Figure 7.1: Symmetric and Full Model a) Symmetric Model b) Full Model

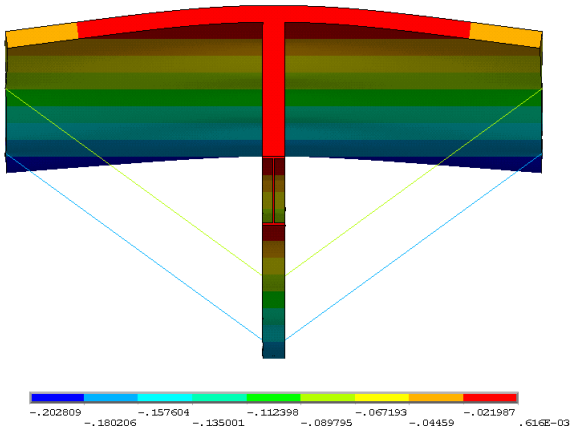

Figure 7.2: Transverse Bending of a Full Panel

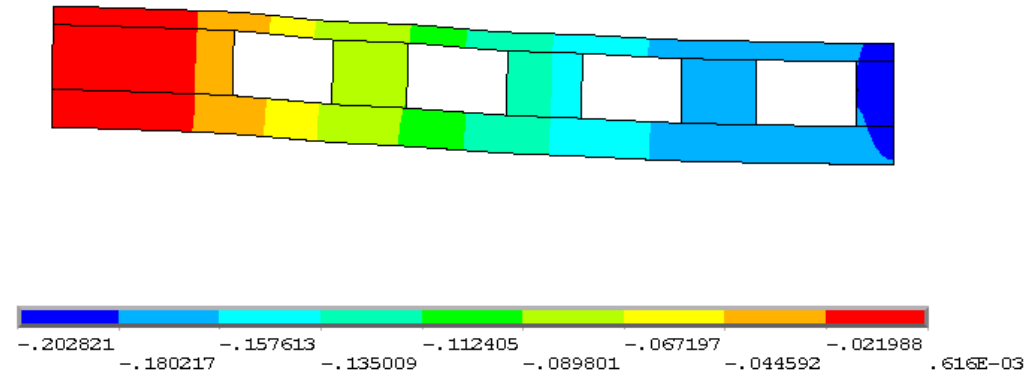

a

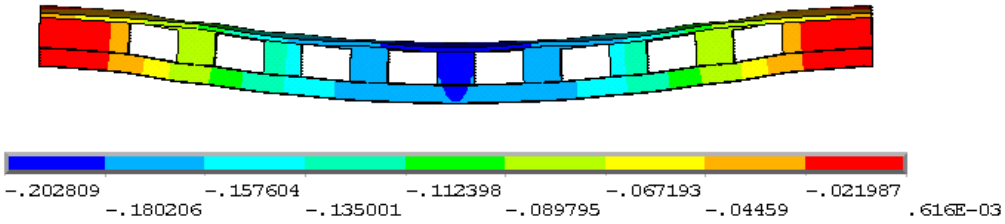

b

Figure 7.3: Comparison of Deflection in in. a) Symmetric Model b) Full Model

Figure 7.4: Stem Wall Cracking (Western Technologies, 2010)

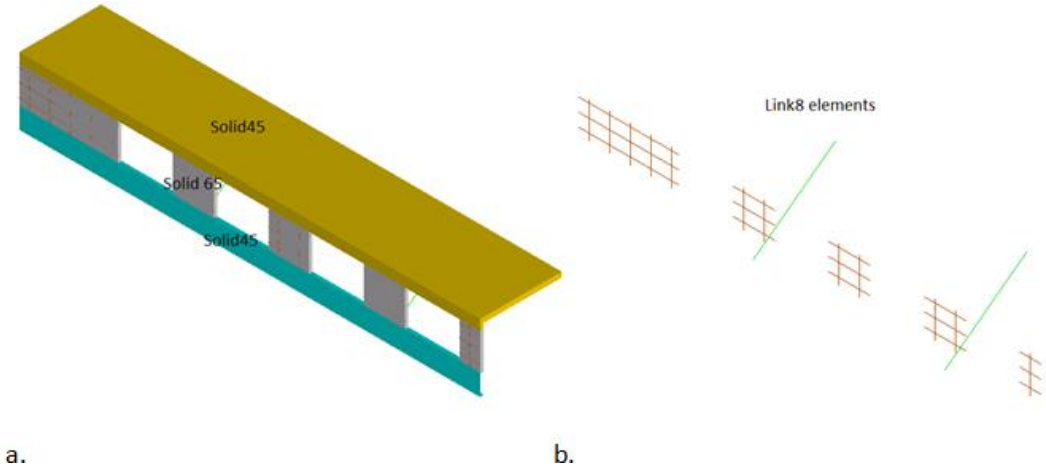

Figure 7.5: Finite Element Model. a) Solid Elements b) Wire Elements

Table 7.1: Material Properties Used in the Finite Element Model

	Steel	Concrete	Units
$f'c$	NA	5.00 e3	psi
Specific weight	2.84 e-1	6.66 e-2	$\frac{\text{lb.}}{\text{in.}^3}$
Density	7.34 e-4	1.72 e-4	$\frac{\frac{\text{lb.}^2}{\text{in.}}}{\text{in.}^3}$
Modulus of Elasticity	2.90 e7	2.74 e6	psi
Poisson's Ratio	0.3	0.2	
Shear Modulus	1.12 e7	1.14 e6	psi

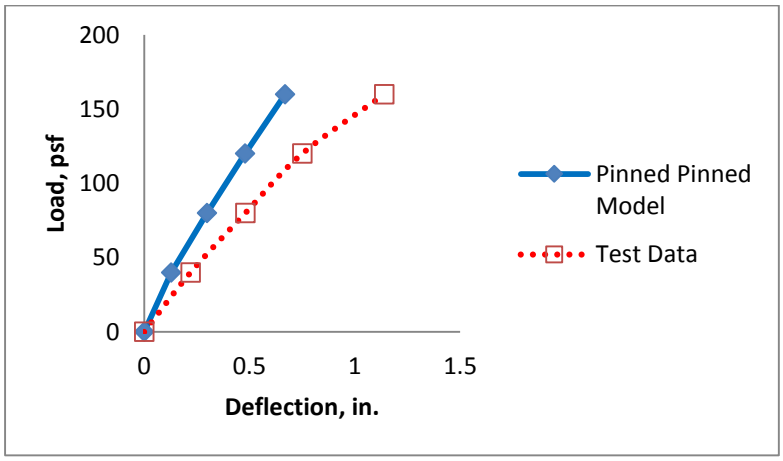

Figure 7.6: Comparison of Pinned-Pinned Model to Test Data

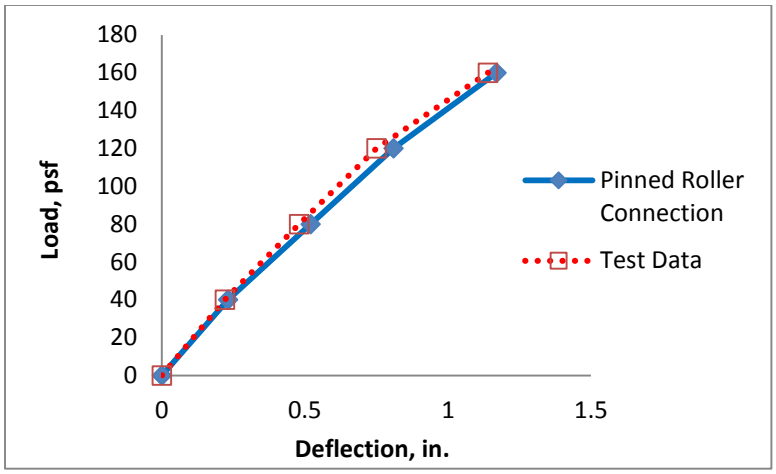

Figure 7.7: Comparison of Pinned-Roller Model to Test Data

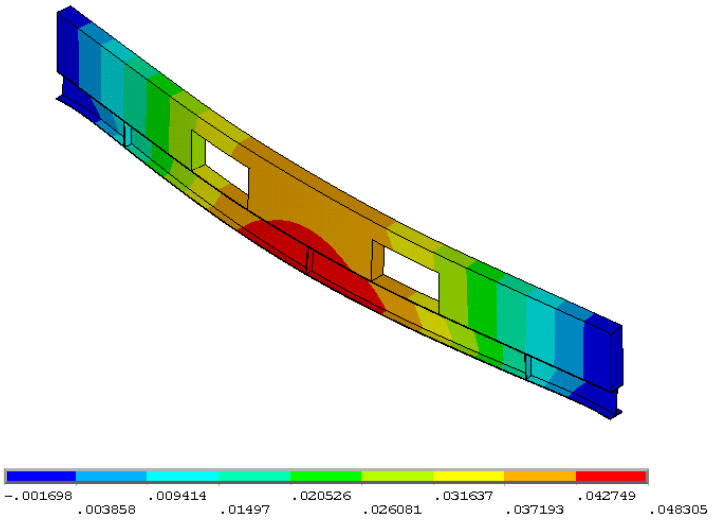

Figure 7.8: Girder Torsional Deflection at Saddle Connection

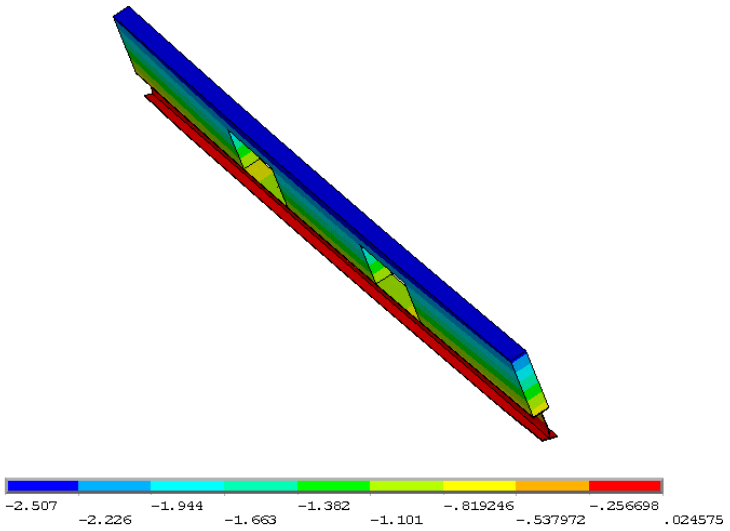

Figure 7.9: Girder Torsional Deflection at Slab Connection

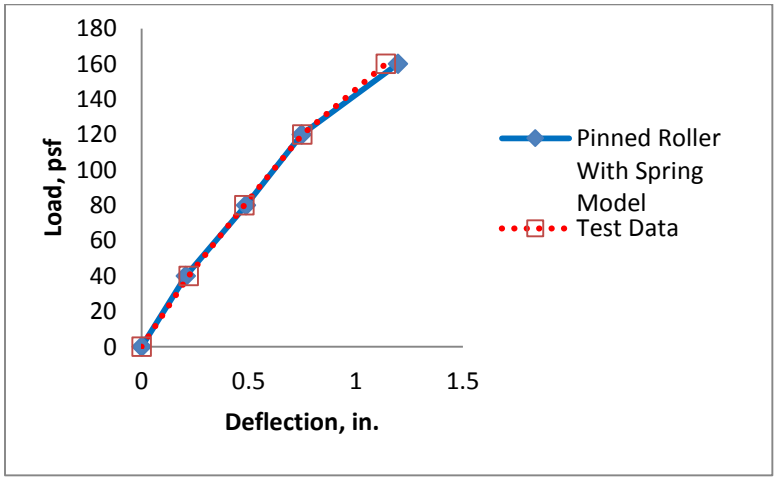

Figure 7.10: Comparison of Pinned-Roller with Spring Model to Test Data

CHAPTER 8

CONSTRUCTED PERFORMANCE BOUNDARY CONDITIONS

The following sections present a method for modeling the boundary conditions of a precast flooring system that reflects the constructed conditions. Section 8.1 describes the various assumptions that can be made for the girder-to-panel connections. Section 8.2 demonstrates a method for modeling the panel-to-panel connections.

8.1 Girder-to-Panel Connections

During the tests at Mountain States Steel, the girder was not connected to columns, nor was the girder loaded on each side. From Chapter 5, Figure 5.2 shows that the girder was simply sitting on pedestals. These pedestals provided no torsional support to the top of the girder. In general, the girder is connected to columns on either side. These columns are connected to the top of the girder by a similar welded plate connection shown in Figure 5.4b. The connection between the column and the girder provides a substantial amount of resistance against torsion.

The slab-to-girder connections and the panel to saddle connection are separated by a distance of more than 3 ft., creating a force couple connection. If panels were connected on opposite sides of the girder, and these panels had similar loads applied to them, the force couple on either side of the girder would cancel out. If there is no net force couple, the girder is braced against rotation.

For this research, the model that reflects the constructed performance of the panels is assumed to be connected to girders that have panels on each side (typical center bay panel). To model the girder boundary conditions, the nodes that reflect the slab-to-girder connections and the panel to saddle connection are prevented from displacing.

8.2 Panel-to-Panel Connections

One alternative to model the panel-to-panel connections is to construct a number of full-size finite element model panels, and connect them together at the appropriate nodes. Unfortunately, this is not feasible with typical computing capabilities. Each panel model is comprised of hundreds of thousands of nodes, each with three degrees of freedom. Modeling more than one panel at a time is computationally expensive. There are, however, ways of analyzing the constructed performance of the panels that are computationally efficient.

The connections between the panels of the Plattform flooring system occur at the brace points. Steel plates are welded across the gap between the two panels along the steel embed plates. If one assumes that the connections behave in a manner such that deflection of one panel at the connection point implies that the connection point of the adjacent panel has the same deflection, the connection can be modeled as a cable substructure.

When the original attempt was made to model the stiffness at the connection points between panels, a set of discrete springs was considered. The stiffness of the springs was calculated by placing a point load over a connection location of a single panel and then analyzing the displacement. After deliberation of this method, it was realized that placing a point load over a single connection point on an actual panel would

result in deflections at the other connection locations. A system of discrete springs at the connection points would not model a substructure in which deflection at a given location would influence the deflection at all other locations. Once this fact was realized, a number of different elements were investigated. The first was a beam element, but calibrating the beam section properties to match the deflection at the discrete connection locations proved impossible. After plotting the deflection at the discrete connection locations, it was found that a simple wire of a given tension showed a deflection plot that most closely corresponded to the deflections of the panel edge at the discrete connection locations. The following paragraphs show how a simple one-dimensional wire element can be used to model deflection at the edge of a panel at discrete connection points.

Suppose one is analyzing panel 1 from the full-scale tests with the condition that the panel is flanked on three sides by a girder, as depicted in Figure 8.1. The locations 1-8 in Figure 8.1 are the connection locations of the panel to the three girders. Numbers 9-12 call out the locations of the panel-to-panel connections. Under the assumptions given in Section 8.1, connections 1-8 are completely locked against any displacement.

The stiffness at points 9-12 can be found by applying arbitrary point loads at these locations and recording the deflection. The deflection at the discrete connection locations found by applying an arbitrary vertical point load of 3000 lbs. at point 10 in ANSYS can be seen in Figure 8.2. Figure 8.2 also compares the deflection of the panel with the deflection of a 45 ft. wire with a tension of 2.37 e6 lbs. As Figure 8.2 exemplifies, the wire has a similar deflection as the panel when given a 3000 lb. load at point 10.

The derivation of the tension in the wire can be found through the second order ordinary differential equation shown in Equation 8.1.

$$T\frac{d^2y}{dx^2} = w(x) \tag{8.1}$$

where T is the tension in the wire, y is the deflection of the wire, x is the location along the wire, and $w(x)$ is the body force applied to the wire. Equation 8.2 can be solved for y using singularity equations.

$$T\frac{d^2y}{dx^2} = P\langle x - a\rangle^{-1} \tag{8.2}$$

where P is the magnitude of the point load, and the Macaulay Brackets are used to define the Dirac Delta function for a point load occurring at a. The following equations solve Equation 8.2 for y.

$$T\frac{d^2y}{dx^2} = P\langle x - a\rangle^{-1} \tag{8.3}$$

$$\Rightarrow \iint d^2y = \iint \frac{P}{T}\langle x - a\rangle^{-1}\, dx^2 \tag{8.4}$$

$$\Rightarrow \int dy = \int \frac{P}{T}(\langle x - a\rangle^{0} + c_1)d_x \tag{8.5}$$

$$\Rightarrow y = \frac{P}{T}(\langle x - a\rangle^{1} + c_1 x + c_2) \tag{8.6}$$

The deflections of $y(0)$ and $y(L)$ are zero, which allows one to find the constants of integration.

$$\Rightarrow y(0) = 0 \Rightarrow c_2 = 0 \tag{8.7}$$

$$\Rightarrow y(L) = 0 = \frac{P}{T}(\langle L - a\rangle^{1} + c_1 L) \Rightarrow c_1 = \frac{(a - L)}{L} \tag{8.8}$$

The deflection of the panel at point 10 in Figure 8.3 is 0.164 in. The slope of the line between the end of the panel, and point 10 under the 3000 lb. load can be found by Equation 8.9.

$$B = \frac{\Delta}{a} = \frac{-0.164}{216} = -7.58\,e-4\,\frac{in.}{in.} \tag{8.9}$$

The wire must follow the same slope if it is to model the stiffness at the connection location, which implies:

$$B = -7.58\,e-4\,\frac{in}{in} = \frac{P}{T}c_1 = \frac{P}{T}\frac{(a-L)}{L} \Rightarrow T = P\,\frac{(a-L)}{-7.58e-4\cdot L} \tag{8.10}$$

$$= 3000\cdot\frac{(216-540)}{-7.58e-4\cdot 540} = 2.37\ e6\ lb. \tag{8.11}$$

Figure 8.2 shows the plot of the wire under a 3000 lb. point load superimposed on the plot of the panel. During the analysis, it was found that for any possible permutation of loads, the ANSYS wire solution closely matched the deflection at the connection locations of the three-dimensional Plattform solution using ANSYS.

Suppose another panel is placed next to the panel in Figure 8.1. This layout is also presented in Figure 8.3. Rather than modeling the girder connected panel as solid elements, the stiffness provided by the first panel at connection points 9-12 can be modeled as a wire. Note that the wire represents the behavior of the panel only at the connection locations that are the locations of compatibility from panel to panel.

Figure 8.4 displays the cable connected configuration. Connecting a cable at points 9-12 allows one to analyze the deflection behavior at connection points 17-20.

Analyzing the stiffness of points 17-20 can be done in the same manner used to find the stiffness of connection points 9-12. If a vertical load of 3000 lbs. is applied to point 18 in Figure 8.4, the deflection of the panel at the connection points can be modeled as a wire with a tension of 1.4e6 lb.

Another panel can then be analyzed, with connection points 17-20 modeled as a cable. This turns into an iterative process. Each cycle places another panel into the system. The Figures 8.5 through 8.9 show that as each additional panel is added to the system, the stiffness provided by the connections begins to converge. Each figure shows the view of the panel system above, then the deflection at the connection locations below. Connection locations 10, 18, 26, 34, and 42 have a 3000 lb. point load placed on them.

Figures 8.5 through 8.9 show that when the third panel is placed in the system, the deflection at the connection points begin to converge as a result of the smaller effect the parallel girder (at points 3-6) has on the central panels. The difference in deflection of the connection points between a three-panel system and a five-panel system is nearly negligible. The tension found for the five-panel condition in the vertical direction is 1.16e6 lb. A similar procedure was used in the horizontal direction, and the converged tension was found to be 4.45e7 lb. If a panel is connected on each side with cables of the aforementioned tensions, the panel behaves similar to a panel in the center of a floor. Figure 8.10 shows the center panel connected to a system of five panels on each side at points 41-48.

The center panel can be connected to wires at locations 41-48 to create the constructed panel-to-panel connections. Figure 8.11 shows the constructed conditions finite element model. Using the model shown in Figure 8.11, the constructed performance of the Plattform system can be analyzed for a number of parameters.

Vibration, asymmetrical loads, various geometrical configurations, and other parameters can be analyzed.

It should be noted that ANSYS does not have a wire or cable element. In order to model the wire connection, one can prestress a Link8 element and turn on geometric nonlinearities. Typically, the one-dimensional Link8 elements can only resist load in the direction of the element. When the geometric nonlinearity feature is used, ANSYS begins an iteration loop where the load is incrementally applied to the system. After each increment in load, the system rechecks the geometry and adjusts stiffness's accordingly. Turning the geometric nonlinearity option on, however, is very computationally expensive.

The Shell181 element with the membrane option turned on can behave as a cable. Adjustments were made to the elements thickness and modulus of elasticity until the stiffness of the Shell181 element matched that of the wire element. Because the stiffness of the Shell181 element is not as intuitive as a wire element, the derivation of the stiffness of the substructure was presented in terms of the wire equation.

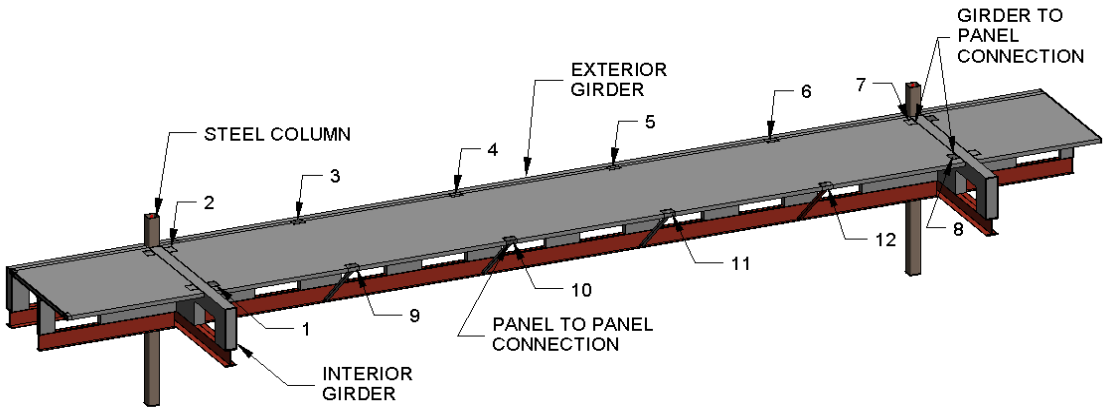

Figure 8.1: Isometric View of a Panel Surrounded on Three Sides by Girders

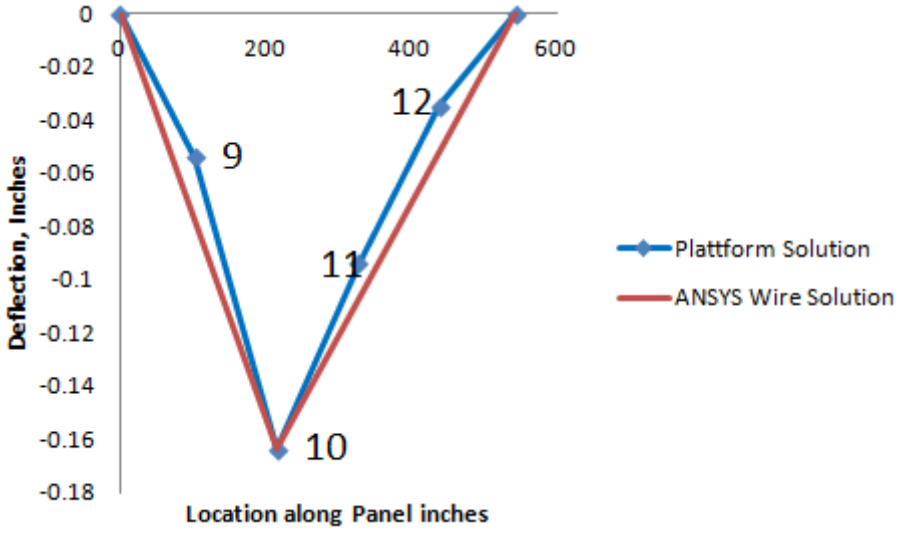

Figure 8.2: Deflection of the Connection Point 10 and a Tensioned Cable

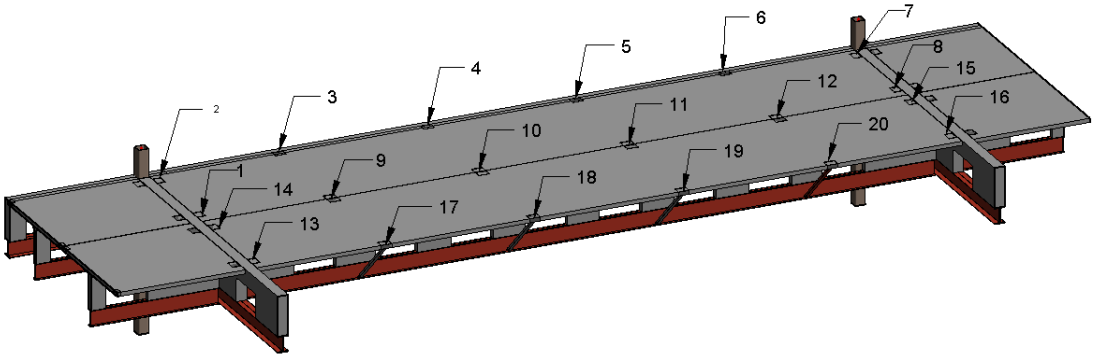

Figure 8.3: Second Panel Connected at Ends by a Girder and Flaked by Another Panel

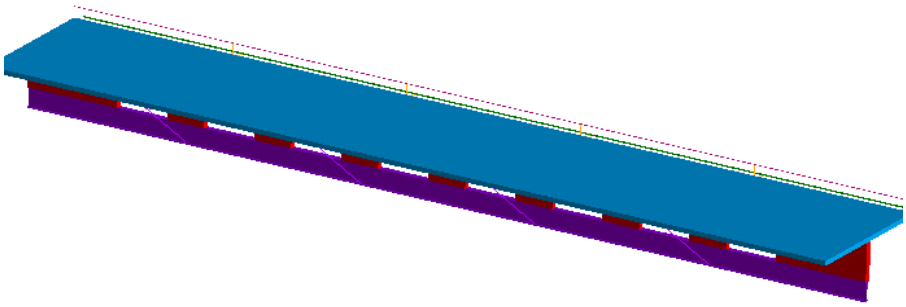

Figure 8.4: Model of Panel with Connection Points 9-12 Modeled as a Tensioned Cable

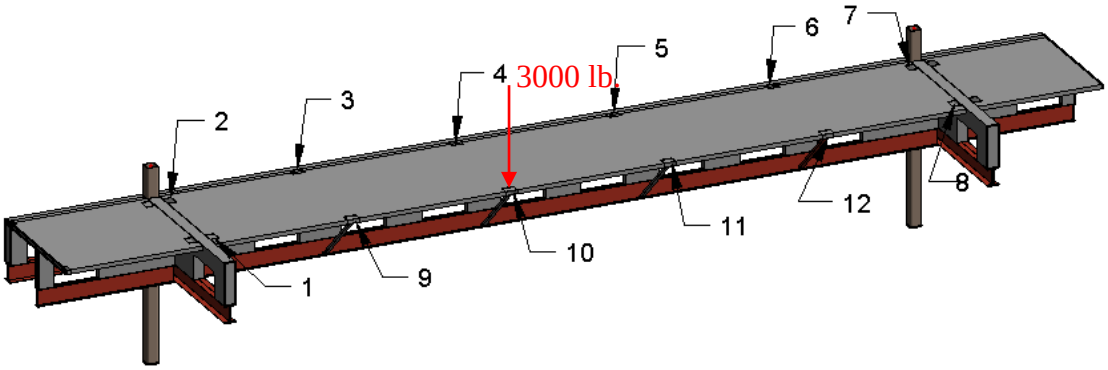

a

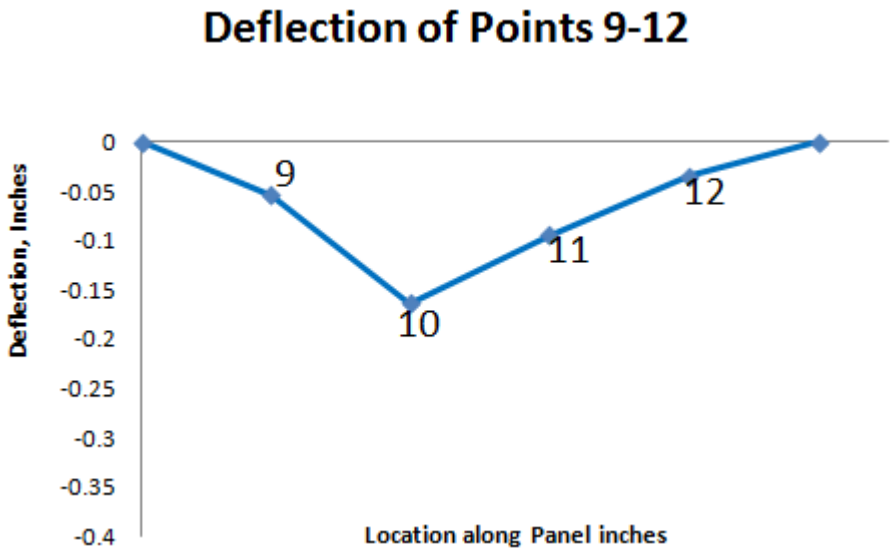

b

Figure 8.5: Single Panel Layout a) Panel Loading b) Deflection of Locations 9-12 with 3000 lb. Load at Point 10

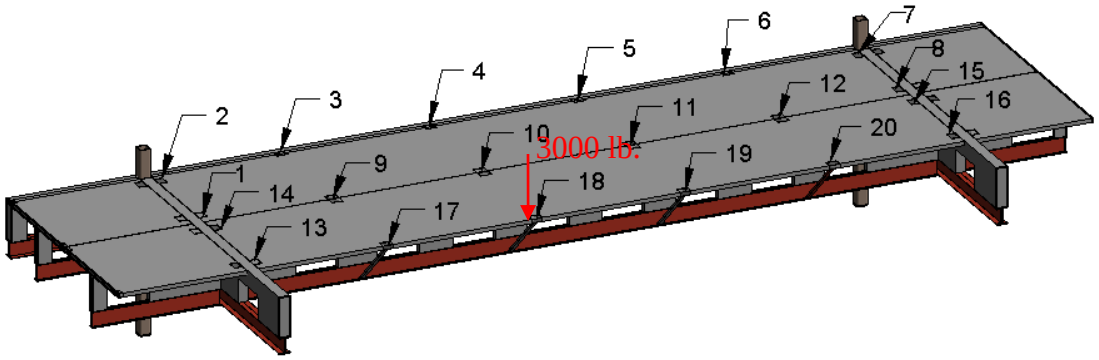

a

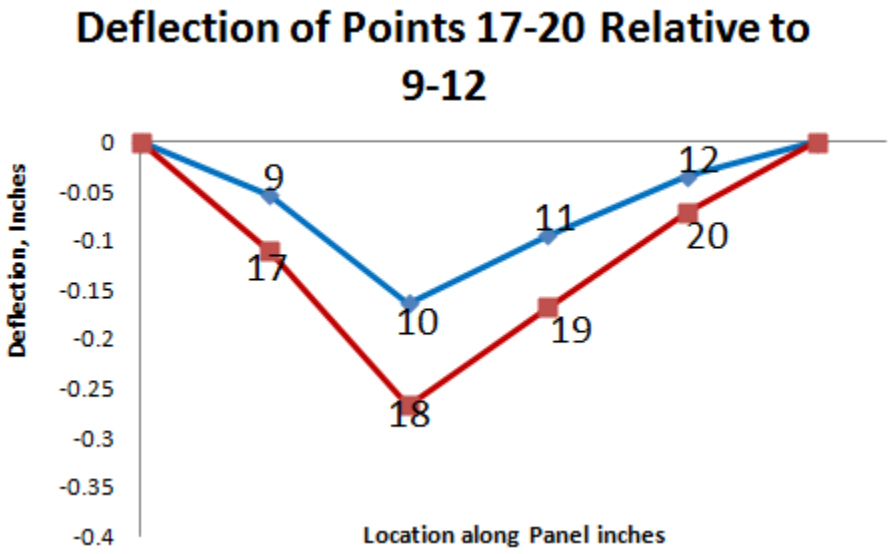

b

Figure 8.6: Two Panel Layout: a) Panel Loading b) Deflection of locations 17-20 with 3000lb. Load at Point 18

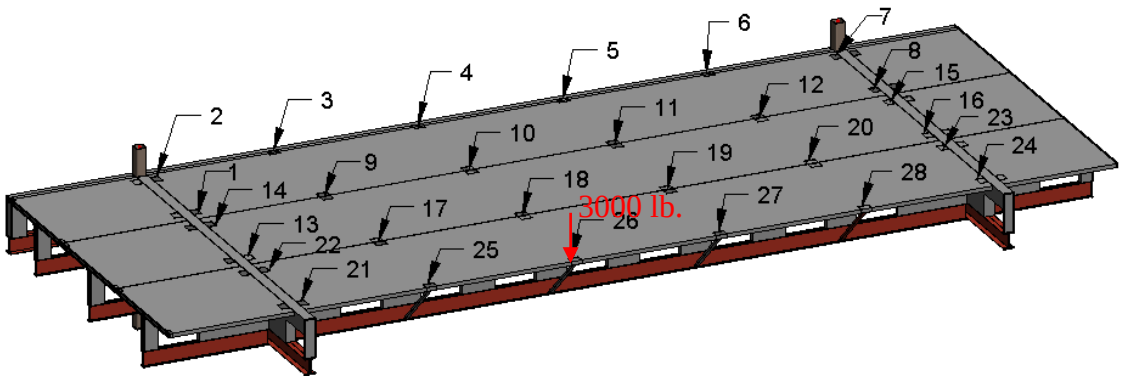

a

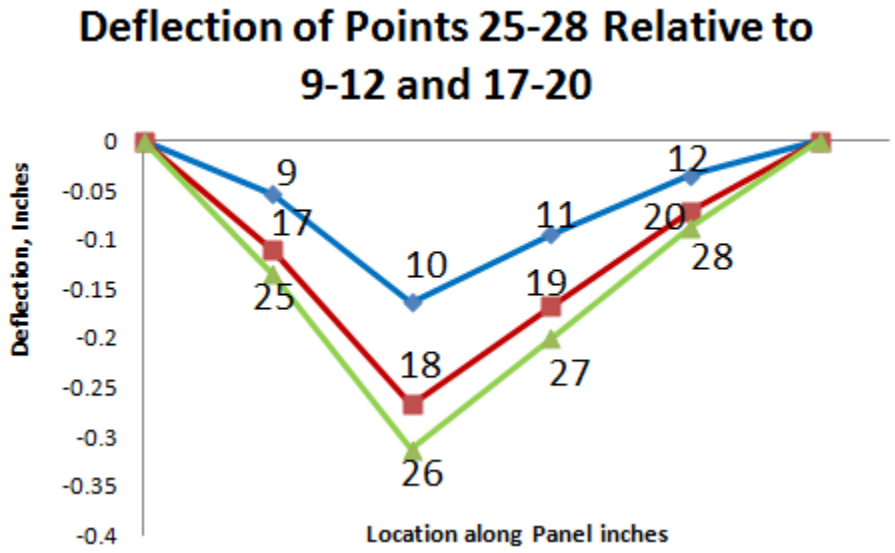

b

Figure 8.7: Three Panel Layout. a) Panel Loading b) Deflection of Locations 25-28 with 3000 lb. Load at Point 26

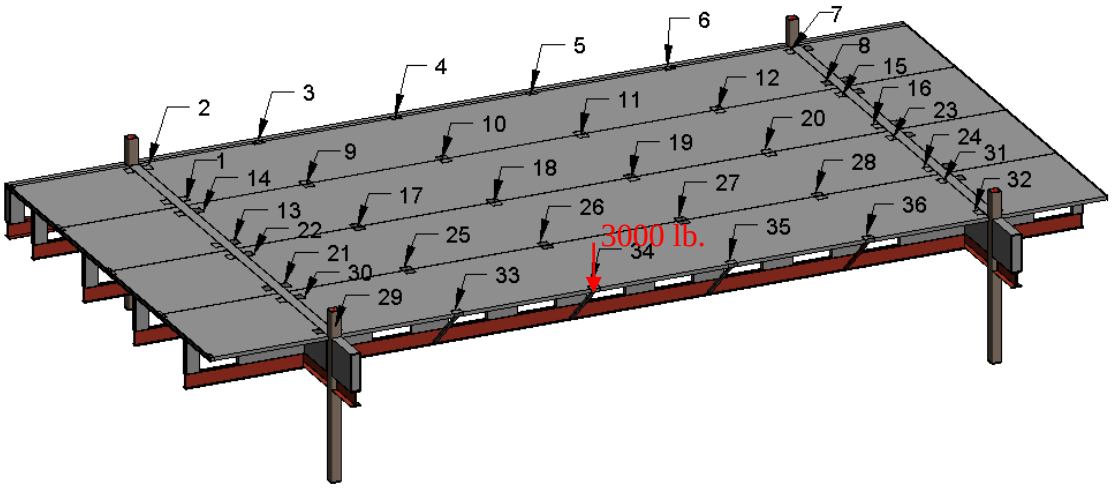

a

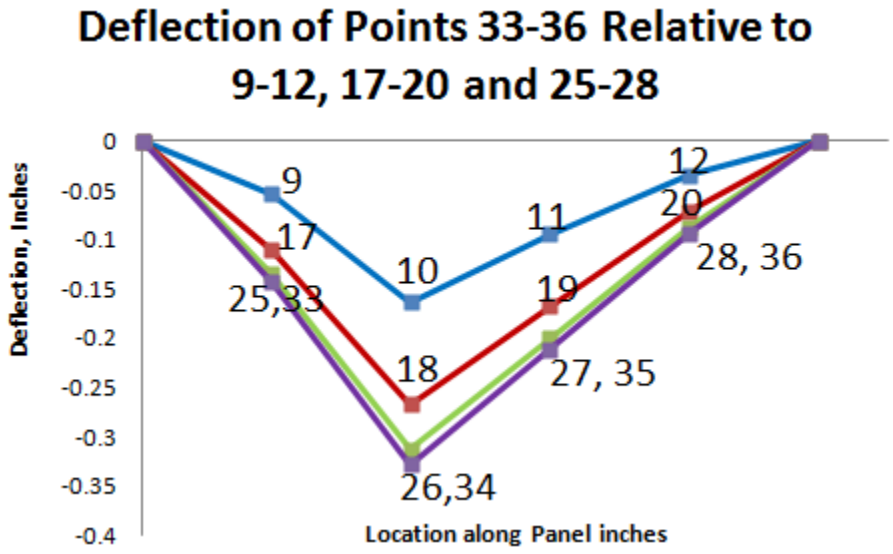

b

Figure 8.8: Four Panel Layout. a) Panel Loading b) Deflection of Locations 33-36 with 3000 lb. Load at Point 34

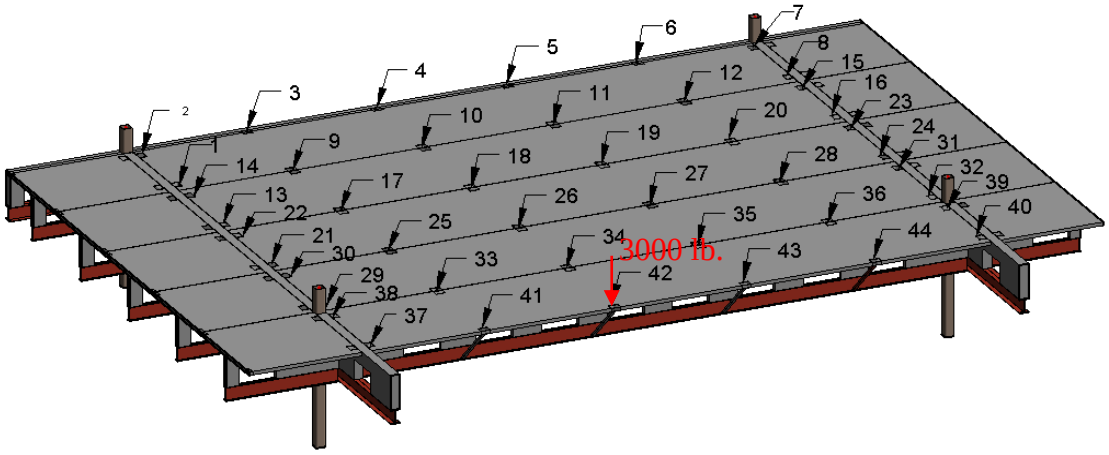

a

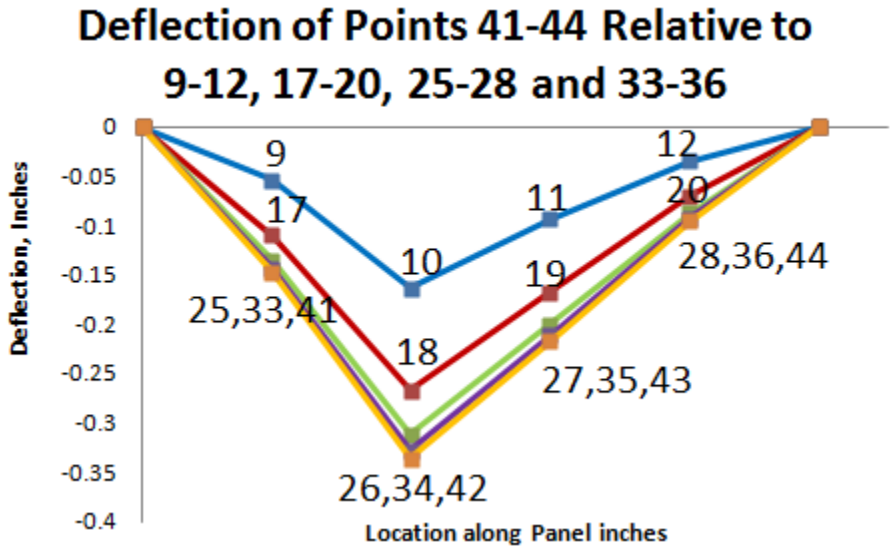

b

Figure 8.9: Five Panel Layout. a) Panel Loading b) Deflection of Locations 41-44 with 3000 lb. Load at Point 42

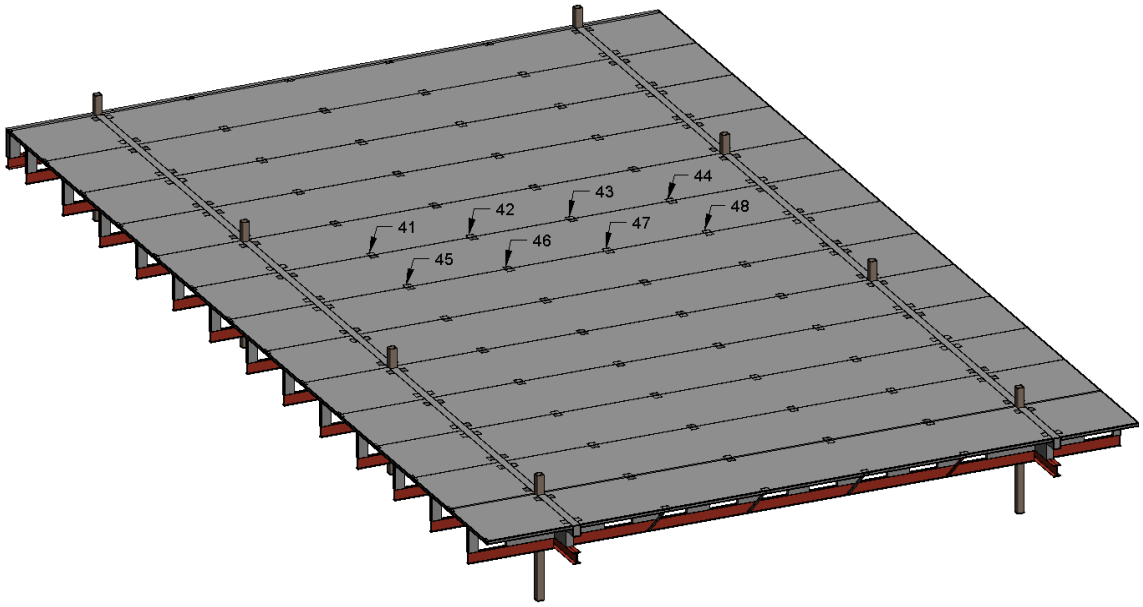

Figure 8.10: Center Floor Panel

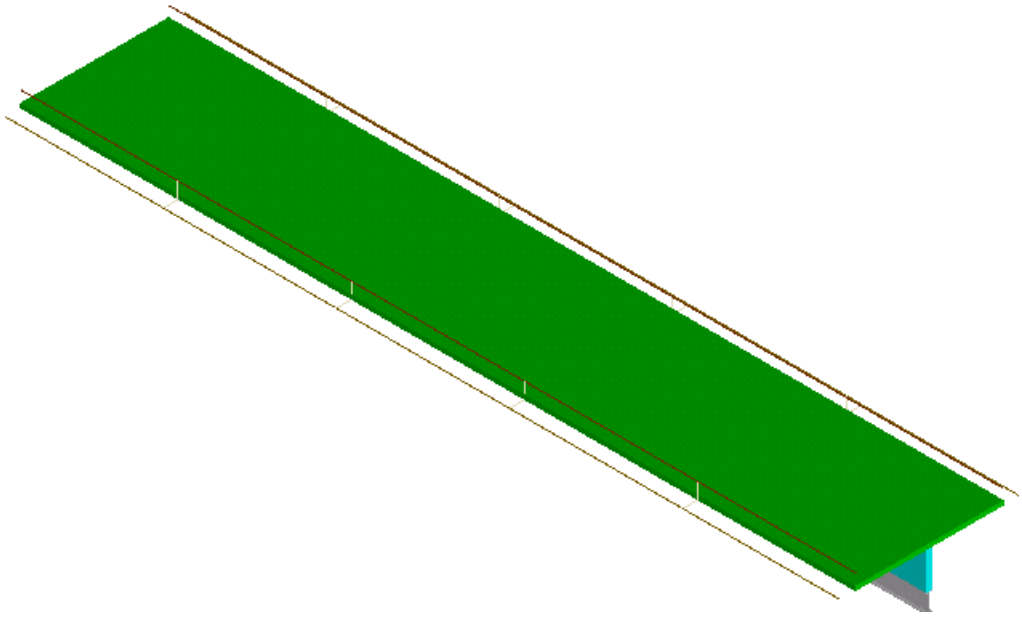

Figure 8.11: Constructed Condition Finite Element Model of a Center Panel

CHAPTER 9

ASYMMETRICAL LOADING ANALYSIS

The current method of analysis used by Plattforms Inc. to analyze the Plattform flooring system is only capable of analyzing uniform loads. The constructed condition model presented in this thesis is a three-dimensional model that can account for various asymmetrical loading conditions. Heavy asymmetrical loads on one panel of the floor have an effect on the behavior of panels in other locations. One should analyze these effects in order to understand the full implications of the floor loading scenario. In his work, Stanton (1992) attempts to define what he calls the "distribution width." As mentioned earlier, this is a qualitative idea that would allow designers to distribute a portion of a concentrated load to adjacent panels. The motivation behind the idea of a distribution width is to reduce the conservative nature of applying a heavy concentrated load to a single panel (Stanton, 1992). The method used to define the effect of a load on adjacent panels for this thesis is done in a very different manner. For the purposes of this section, the term "loaded panel" is used to define a panel that has an arbitrary concentrated load somewhere on the panel. The term "adjacent panel" is used to define a panel that is connected to the "loaded panel" at the connection locations. The term "selected panel" refers to the panel in a floor plan that has been selected for analysis. The term "concentrated load" is used to define an area load that occurs in a given location of a panel but does not cover the entire panel. The term "point load" is used to define a load

that occurs at a discrete point on the panel.

For this thesis, the method of analyzing the effects of loads to adjacent panels is as follows:

1. Apply a concentrated load to a constructed condition panel (the loaded panel).
2. Record the deflection at the connection points of the loaded panel.
3. Calculate the magnitude of the point loads that must be applied at the connection locations of an unloaded adjacent panel in order to match the deflections at the connection locations for the panel under a concentrated load using a 4× 4 stiffness matrix. Note that only the deflections on one side of the adjacent panel are known at this time.
4. Calculate the unknown deflection at the other connection locations on the adjacent panel using an 8× 8 compliance matrix.
5. Steps 2-4 can be repeated to calculate the effects on a selected panel of a floor system.

Step 1 is fairly straightforward. The constructed conditions panel finite element model has already been created. Applying an area load to that model is a simple task. Step 2 is also simple, as ANSYS can find the nodal displacements anywhere in the model. Step 3 is slightly more involved. When the loaded panel deflects under the concentrated load, the substructure deflects as well. Remember that the substructure represents the adjacent panel connections. Therefore, the adjacent panel has a prescribed displacement. The displacements of the connection locations joining the loaded panel, and the adjacent panel are known from the analysis of the loaded panel. One can prescribe the known displacements in the adjacent panel by applying appropriate point loads to an unloaded constructed conditions finite element model at the connection

locations. These point loads can be found through a 4×4 stiffness matrix. The point loads required to displace the connection locations of the adjacent panel can then be applied directly to the unloaded constructed conditions finite element model. The loading scenario of the adjacent panel can be run, and the deflections of the other connection locations can be found. This is a fairly cumbersome and unnecessary process. Once the point loads required to obtain the appropriate displacements at the adjacent panel connection locations on one side are known, an 8×8 compliance matrix can then be used to calculate the unknown deflections at the connection locations of the adjacent panel.

The preceding paragraph has been a qualitative introduction into the work that was done to try to understand the effect loading a single panel has on adjacent panels. The following sections show how the compliance and stiffness matrices are created, and how they can be used for different types of analysis. Section 9.1 describes how the stiffness and compliance matrices are created. Section 9.2 shows how the stiffness and compliance matrices can be used to quantify the effect loading one panel has on the adjacent panels. Section 9.3 discusses how the loads dissipate across the floor system.

9.1 Stiffness and Compliance Matrices of Connection Locations

There are 8 panel-to-panel connection locations on each panel. Applying a load at a given connection results in deflections at all 8 locations. The deflections can then be used to determine the compliance vector of the connection that is loaded. A load can be applied over each of the connection locations to create a compliance matrix of the panel connections. The following derivation describes the method used to find the compliance matrix of a single Plattform panel.

There are 8 connection locations; for all practical purposes, only the deflection in

the vertical direction is relevant. Eight locations and only one degree of freedom per location implies that the compliance matrix is an 8×8 matrix. Equation 9.1 displays the compliance force equation.

$$\begin{bmatrix} X_1 \\ X_2 \\ X_3 \\ X_4 \\ X_5 \\ X_6 \\ X_7 \\ X_8 \end{bmatrix} = \begin{bmatrix} m_{1,1} & m_{1,2} & m_{1,3} & m_{1,4} & m_{1,5} & m_{1,6} & m_{1,7} & m_{1,8} \\ m_{2,1} & m_{2,2} & m_{2,3} & m_{2,4} & m_{2,5} & m_{2,6} & m_{2,7} & m_{2,8} \\ m_{3,1} & m_{3,2} & m_{3,3} & m_{3,4} & m_{3,5} & m_{3,6} & m_{3,7} & m_{3,8} \\ m_{4,1} & m_{4,2} & m_{4,3} & m_{4,4} & m_{4,5} & m_{4,6} & m_{4,7} & m_{4,8} \\ m_{5,1} & m_{5,2} & m_{5,3} & m_{5,4} & m_{5,5} & m_{5,6} & m_{5,7} & m_{5,8} \\ m_{6,1} & m_{6,2} & m_{6,3} & m_{6,4} & m_{6,5} & m_{6,6} & m_{6,7} & m_{6,8} \\ m_{7,1} & m_{7,2} & m_{7,3} & m_{7,4} & m_{7,5} & m_{7,6} & m_{7,7} & m_{7,8} \\ m_{8,1} & m_{8,2} & m_{8,3} & m_{8,4} & m_{8,5} & m_{8,6} & m_{8,7} & m_{8,8} \end{bmatrix} \begin{bmatrix} F_1 \\ F_2 \\ F_3 \\ F_4 \\ F_5 \\ F_6 \\ F_7 \\ F_8 \end{bmatrix} \tag{9.1}$$

where the X vector is the displacement of the connections, the m matrix is the compliance matrix, and the F vector is the force vector applied at the connection locations. Figure 9.1 shows the constructed conditions model with connection locations 1-8.

The vectors of the compliance matrix can be found by applying a force to only a single connection location of the constructed conditions model, running the simulation in ANSYS, and recording the results.

Equation 9.2 shows the resultant equation of only the F1 force being applied to connection location 1. The F1 force can be applied to the constructed condition model, and the deflections at each of the 8 connection locations can be found from ANSYS. The compliance vector associated with this connection location can then be found by dividing the deflections at each of these locations by the force F1. Equation 9.2 shows how this can be done with a 3000 lb. point load.

$$\begin{bmatrix} X_1 \\ X_2 \\ X_3 \\ X_4 \\ X_5 \\ X_6 \\ X_7 \\ X_8 \end{bmatrix} = \begin{bmatrix} m_{1,1} \\ m_{2,1} \\ m_{3,1} \\ m_{4,1} \\ m_{5,1} \\ m_{6,1} \\ m_{7,1} \\ m_{8,1} \end{bmatrix} F_1 = \begin{bmatrix} -1.03\ e-1 \\ -7.59\ e-2 \\ -4.94\ e-2 \\ -2.24\ e-2 \\ 6.23\ e-2 \\ 5.08\ e-2 \\ 3.34\ e-2 \\ 1.66\ e-2 \end{bmatrix} \text{in} = \begin{bmatrix} m_{1,1} \\ m_{2,1} \\ m_{3,1} \\ m_{4,1} \\ m_{5,1} \\ m_{6,1} \\ m_{7,1} \\ m_{8,1} \end{bmatrix} \cdot -3000\ \text{lbs}$$

$$\Rightarrow \begin{bmatrix} m_{1,1} \\ m_{2,1} \\ m_{3,1} \\ m_{4,1} \\ m_{5,1} \\ m_{6,1} \\ m_{7,1} \\ m_{8,1} \end{bmatrix} = \begin{bmatrix} -1.03\ e-1 \\ -7.59\ e-2 \\ -4.94\ e-2 \\ -2.24\ e-2 \\ 6.23\ e-2 \\ 5.08\ e-2 \\ 3.34\ e-2 \\ 1.66\ e-2 \end{bmatrix} \cdot \frac{1}{-3000\text{lbs}} = \begin{bmatrix} 3.42\ e-5 \\ 2.53\ e-5 \\ 1.65\ e-5 \\ 7.47\ e-6 \\ -2.08\ e-5 \\ -1.69\ e-5 \\ -1.11\ e-5 \\ -5.54\ e-6 \end{bmatrix} \frac{\text{in}}{\text{lbs}} \tag{9.2}$$

Similarly, the second vector of the compliance matrix can be found.

$$\begin{bmatrix} X_1 \\ X_2 \\ X_3 \\ X_4 \\ X_5 \\ X_6 \\ X_7 \\ X_8 \end{bmatrix} = \begin{bmatrix} m_{1,2} \\ m_{2,2} \\ m_{3,2} \\ m_{4,2} \\ m_{5,2} \\ m_{6,2} \\ m_{7,2} \\ m_{8,2} \end{bmatrix} F_2 = \begin{bmatrix} -7.59\ e-2 \\ -1.66\ e-1 \\ -1.08\ e-1 \\ -4.94\ e-2 \\ 5.08\ e-2 \\ 9.53\ e-2 \\ 6.68\ e-2 \\ 3.34\ e-2 \end{bmatrix} \text{in} = \begin{bmatrix} m_{1,2} \\ m_{2,2} \\ m_{3,2} \\ m_{4,2} \\ m_{5,2} \\ m_{6,2} \\ m_{7,2} \\ m_{8,2} \end{bmatrix} \cdot -3000\text{lbs}$$

$$\Rightarrow \begin{bmatrix} m_{1,1} \\ m_{2,1} \\ m_{3,1} \\ m_{4,1} \\ m_{5,1} \\ m_{6,1} \\ m_{7,1} \\ m_{8,1} \end{bmatrix} = \begin{bmatrix} -7.59\ e-2 \\ -1.66\ e-1 \\ -1.08\ e-1 \\ -4.94\ e-2 \\ 5.08\ e-2 \\ 9.53\ e-2 \\ 6.68\ e-2 \\ 3.34\ e-2 \end{bmatrix} \cdot \frac{1}{-3000\text{lbs}} = \begin{bmatrix} 2.53\ e-5 \\ 5.44\ e-5 \\ 3.61\ e-5 \\ 1.65\ e-5 \\ -1.69\ e-5 \\ -3.18\ e-5 \\ -2.23\ e-5 \\ -1.11\ e-5 \end{bmatrix} \tag{9.3}$$

Due to the symmetry of the system, all other columns of the compliance matrix can be found by rearranging the two columns shown in 9.2 and 9.3. The final compliance matrix is shown in Equation 9.4.

$$\boldsymbol{m} = \begin{bmatrix} 3.42\,e-5 & 2.53\,e-5 & 1.65\,e-5 & 7.47\,e-6 & -2.08\,e-5 & -1.69\,e-5 & -1.11\,e-5 & -5.54\,e-6 \\ 2.53\,e-5 & 5.54\,e-5 & 3.61\,e-5 & 1.65\,e-5 & -1.69\,e-5 & -3.18\,e-5 & -2.23\,e-5 & -1.11\,e-5 \\ 1.65\,e-5 & 3.61\,e-5 & 5.54\,e-5 & 2.53\,e-5 & -1.11\,e-5 & -2.23\,e-5 & -3.18\,e-5 & -1.69\,e-5 \\ 7.47\,e-6 & 1.65\,e-5 & 2.53\,e-5 & 3.42\,e-5 & -5.54\,e-6 & -1.11\,e-5 & -1.69\,e-5 & -2.08\,e-5 \\ -2.08\,e-5 & -1.69\,e-5 & -1.11\,e-5 & -5.54\,e-6 & 3.42\,e-5 & 2.53\,e-5 & 1.65\,e-5 & 7.47\,e-6 \\ -1.69\,e-5 & -3.18\,e-5 & -2.23\,e-5 & -1.11\,e-5 & 2.53\,e-5 & 5.54\,e-5 & 3.61\,e-5 & 1.65\,e-5 \\ -1.11\,e-5 & -2.23\,e-5 & -3.18\,e-5 & -1.69\,e-5 & 1.65\,e-5 & 3.61\,e-5 & 5.54\,e-5 & 2.53\,e-5 \\ -5.54\,e-6 & -1.11\,e-5 & -1.69\,e-5 & -2.08\,e-5 & 7.47\,e-6 & 1.65\,e-5 & 2.53\,e-5 & 3.42\,e-5 \end{bmatrix} \frac{\text{in}}{\text{lb}} \tag{9.4}$$

The first 4 rows and 4 columns of the compliance matrix shown in Equation 9.4 create a 4x4 compliance matrix for one side of the Plattform panel, and is shown in Equation 9.5. The $\boldsymbol{m_{4x4}}$ matrix can then be inverted to create a 4x4 stiffness matrix that defines the stiffness at the connection locations of a single side of a constructed conditions panel.

$$\mathbf{m_{4x4}} = \begin{bmatrix} 3.42\text{ e}-5 & 2.53\text{ e}-5 & 1.65\text{ e}-5 & 7.47\text{ e}-6 \\ 2.53\text{ e}-5 & 5.54\text{ e}-5 & 3.61\text{ e}-5 & 1.65\text{ e}-5 \\ 1.65\text{ e}-5 & 3.61\text{ e}-5 & 5.54\text{ e}-5 & 2.53\text{ e}-5 \\ 7.47\text{ e}-6 & 1.65\text{ e}-5 & 2.53\text{ e}-5 & 3.42\text{ e}-5 \end{bmatrix} \frac{\text{in.}}{\text{lb.}} \tag{9.5}$$

$$\boldsymbol{k_{4x4}} = \boldsymbol{m_{4x4}}^{-1} = \begin{bmatrix} 44193 & -20211 & 12.29 & 63.61 \\ -20211 & 40611 & -20460 & 12.29 \\ 12.29 & -20460 & 40611 & -20211 \\ 63.61 & 12.29 & -20211 & 44193 \end{bmatrix} \frac{\text{lb.}}{\text{in.}} \tag{9.6}$$

9.2 Use of the Stiffness and Compliance Matrices of Connection Locations

The stiffness and compliance matrices can be used to analyze the effect a concentrated load on a single panel has on the adjacent panels of a floor system. A floor may be subject to a heavy 12 psi concentrated load configuration like that shown in Figure 9.2. Panel 6 has both a heavy longitudinal line load, and a heavy transverse line load. This panel is the selected panel for the flooring system. One could simply analyze the effect of loading the selected panel by placing both the longitudinal and transverse line loads on the constructed conditions panel, and running the simulation in ANSYS; however, that would not reflect the effects of the loads given from panels 1-5. In order to analyze the entire flooring system, the effect loading a single panel has on the adjacent

panels must be understood. Suppose one would like to analyze the effect of loading the far left panel (panel 1) in Figure 9.2 on the next five panels. If only panel 1 is loaded, the deflection created by the concentrated load creates a deflection on the panel directly to the right (panel 2) at the four connection locations shared by panels 1 and 2. The downward deflection at the left four connection locations on panel 2 in turn creates an upward deflection at the right four connection locations of panel 2. The deflections propagate across the flooring system through the compatibility of the connection locations. Figure 9.3 depicts the deflections of each of the adjacent panels due to the 12 psi load on panel 1. These deflections were found using the compliance and stiffness matrices defined in this chapter. The following derivation shows how this is done.

The steps involved in the procedure were defined in the beginning of this chapter, and are restated here for clarity:

1. Apply a concentrated load to a constructed condition panel.
2. Record the deflection at the connection points of the loaded panel.
3. Calculate the magnitude of the point loads that must be applied at the connection locations of an unloaded adjacent panel in order to match the deflections at the connection locations for the panel under a concentrated load using a 4× 4 stiffness matrix. Note that only the deflections on one side of the adjacent panel are known at this time.
4. Calculate the unknown deflection at the other connection locations on the adjacent panel using an 8× 8 compliance matrix.
5. Steps 2-4 can be repeated to calculate the effects on a selected panel of a floor system.

The deflections at the connection locations for panel 1 were found by applying the

concentrated load to the constructed conditions model in ANSYS, and running the simulation. As described earlier, these deflections also represent the deflections of the adjacent panel (panel 2). Although panel 2 does not have a concentrated load applied to it, it does have a prescribed displacement from the load on panel 1. The prescribed displacement can be created by applying point loads at the connection locations of panel 2. The magnitude of these point loads can be found using the stiffness matrix defined in Equation 9.6. Equation 9.7 displays this event.

$$\mathbf{F} = \mathbf{k_{4x4}X} = \begin{bmatrix} 44193 & -20211 & 12.29 & 63.61 \\ -20211 & 40611 & -20460 & 12.29 \\ 12.29 & -20460 & 40611 & -20211 \\ 63.61 & 12.29 & -20211 & 44193 \end{bmatrix} \begin{bmatrix} -0.31\,\mathrm{e}-1 \\ -0.81\,\mathrm{e}-1 \\ -0.81\,\mathrm{e}-1 \\ -0.31\,\mathrm{e}-1 \end{bmatrix} = \begin{bmatrix} 264.5 \\ -1000 \\ -1000 \\ 264.5 \end{bmatrix} \text{ lb.} \quad (9.7)$$

By applying the forces shown in Equation 9.7 to the left connection locations of panel 2, panel 2 has the deflections shown in Figure 9.3. At this time, however, only the deflections at the left connection locations of panel 2 are known. The compliance matrix can then be used to calculate the deflections at the right connection locations of panel 2, as shown in Equation 9.8.

$$\boldsymbol{X} = \boldsymbol{mF} = \begin{bmatrix} 3.4e-5 & 2.5e-5 & 1.7e-5 & 7.5e-6 & -2.1e-5 & -1.7e-5 & -1.1e-5 & -5.5e-6 \\ 2.5e-5 & 5.5e-5 & 3.6e-5 & 1.7e-5 & -1.7e-5 & -3.2e-5 & -2.2e-5 & -1.1e-5 \\ 1.7e-5 & 3.6e-5 & 5.5e-5 & 2.5e-5 & -1.1e-5 & -2.2e-5 & -3.7e-5 & -1.7e-5 \\ 7.5e-6 & 1.7e-5 & 2.5e-5 & 3.4e-5 & -5.5e-6 & -1.1e-5 & -1.7e-5 & -2.1e-5 \\ -2.1e-5 & -1.7e-5 & -1.1e-5 & -5.5e-6 & 3.4e-5 & 2.5e-5 & 1.7e-5 & 7.5e-6 \\ -1.7e-5 & -3.2e-5 & -2.2e-5 & -1.1e-5 & 2.5e-5 & 5.5e-5 & 3.6e-5 & 1.7e-5 \\ -1.1e-5 & -2.2e-5 & -3.2e-5 & -1.7e-5 & 1.7e-5 & 3.6e-5 & 5.5e-5 & 2.5e-5 \\ -5.5e-6 & -1.1e-5 & -1.7e-5 & -2.1e-5 & 7.5e-6 & 1.7e-5 & 2.5e-5 & 3.4e-5 \end{bmatrix} \begin{bmatrix} 264.5 \\ -1000 \\ -1000 \\ 264.5 \\ 0 \\ 0 \\ 0 \\ 0 \end{bmatrix} = \begin{bmatrix} -0.31e-1 \\ -0.81e-1 \\ -0.81e-1 \\ -0.31e-1 \\ 0.21e-1 \\ 0.47e-1 \\ 0.47e-1 \\ 0.21e-1 \end{bmatrix} \text{in..} \quad (9.8)$$

The last 4 entries of the displacement vector give the displacement of the right connection points of panel 2. The preceding process can then be repeated to find the deflections of panel 3.

The deflections of the left connection points of panel 3 are now known. The

stiffness matrix from Equation 9.6 can now be used again with the displacement vector as the last 4 entries of the displacement vector from 9.8.

$$\boldsymbol{F} = \boldsymbol{k_{4x4}X} = \begin{bmatrix} 44193 & -20211 & 12.29 & 63.61 \\ -20211 & 40611 & -20460 & 12.29 \\ 12.29 & -20460 & 40611 & -20211 \\ 63.61 & 12.29 & -20211 & 44193 \end{bmatrix} \begin{bmatrix} 0.21\,e-1 \\ 0.47\,e-1 \\ 0.47\,e-1 \\ 0.21\,e-1 \end{bmatrix} = \begin{bmatrix} -20 \\ 523 \\ 523 \\ -20 \end{bmatrix} \text{lb.} \quad (9.9)$$

The 8x8 compliance matrix can then be used to calculate the deflections of the right connection locations of panel 3:

$$\boldsymbol{X} = \boldsymbol{mF} = \begin{bmatrix} 3.4\,e-5 & 2.5\,e-5 & 1.7\,e-5 & 7.5\,e-6 & -2.1\,e-5 & -1.7\,e-5 & -1.1\,e-5 & -5.5\,e-6 \\ 2.5\,e-5 & 5.5\,e-5 & 3.6\,e-5 & 1.7\,e-5 & -1.7\,e-5 & -3.2\,e-5 & -2.2\,e-5 & -1.1\,e-5 \\ 1.7\,e-5 & 3.6\,e-5 & 5.5\,e-5 & 2.5\,e-5 & -1.1\,e-5 & -2.2\,e-5 & -3.7\,e-5 & -1.7\,e-5 \\ 7.5\,e-6 & 1.7\,e-5 & 2.5\,e-5 & 3.4\,e-5 & -5.5\,e-6 & -1.1\,e-5 & -1.7\,e-5 & -2.1\,e-5 \\ -2.1\,e-5 & -1.7\,e-5 & -1.1\,e-5 & -5.5\,e-6 & 3.4\,e-5 & 2.5\,e-5 & 1.7\,e-5 & 7.5\,e-6 \\ -1.7\,e-5 & -3.2\,e-5 & -2.2\,e-5 & -1.1\,e-5 & 2.5\,e-5 & 5.5\,e-5 & 3.6\,e-5 & 1.7\,e-5 \\ -1.1\,e-5 & -2.2\,e-5 & -3.2\,e-5 & -1.7\,e-5 & 1.7\,e-5 & 3.6\,e-5 & 5.5\,e-5 & 2.5\,e-5 \\ -5.5\,e-6 & -1.1\,e-5 & -1.7\,e-5 & -2.1\,e-5 & 7.5\,e-6 & 1.7\,e-5 & 2.5\,e-5 & 3.4\,e-5 \end{bmatrix} \begin{bmatrix} -20 \\ 523 \\ 523 \\ -20 \\ 0 \\ 0 \\ 0 \\ 0 \end{bmatrix} = \begin{bmatrix} 0.21\,e-1 \\ 0.47\,e-1 \\ 0.47\,e-1 \\ 0.21\,e-1 \\ -0.14\,e-1 \\ -0.28\,e-1 \\ -0.28\,e-1 \\ -0.14\,e-1 \end{bmatrix} \text{in.} \quad (9.10)$$

This process can be repeated as shown in the following equations.

Loads to apply to left connections of panel 4:

$$\boldsymbol{F} = \boldsymbol{k_{4x4}X} = \begin{bmatrix} 44193 & -20211 & 12.29 & 63.61 \\ -20211 & 40611 & -20460 & 12.29 \\ 12.29 & -20460 & 40611 & -20211 \\ 63.61 & 12.29 & -20211 & 44193 \end{bmatrix} \begin{bmatrix} -0.14\,e-1 \\ -0.28\,e-1 \\ -0.28\,e-1 \\ -0.14\,e-1 \end{bmatrix} = \begin{bmatrix} -54 \\ -281 \\ -281 \\ -54 \end{bmatrix} \text{lb.} \quad (9.11)$$

Deflections of connection locations of panel 4:

$$\boldsymbol{X} = \boldsymbol{mF} = \begin{bmatrix} 3.4\,e-5 & 2.5\,e-5 & 1.7\,e-5 & 7.5\,e-6 & -2.1\,e-5 & -1.7\,e-5 & -1.1\,e-5 & -5.5\,e-6 \\ 2.5\,e-5 & 5.5\,e-5 & 3.6\,e-5 & 1.7\,e-5 & -1.7\,e-5 & -3.2\,e-5 & -2.2\,e-5 & -1.1\,e-5 \\ 1.7\,e-5 & 3.6\,e-5 & 5.5\,e-5 & 2.5\,e-5 & -1.1\,e-5 & -2.2\,e-5 & -3.7\,e-5 & -1.7\,e-5 \\ 7.5\,e-6 & 1.7\,e-5 & 2.5\,e-5 & 3.4\,e-5 & -5.5\,e-6 & -1.1\,e-5 & -1.7\,e-5 & -2.1\,e-5 \\ -2.1\,e-5 & -1.7\,e-5 & -1.1\,e-5 & -5.5\,e-6 & 3.4\,e-5 & 2.5\,e-5 & 1.7\,e-5 & 7.5\,e-6 \\ -1.7\,e-5 & -3.2\,e-5 & -2.2\,e-5 & -1.1\,e-5 & 2.5\,e-5 & 5.5\,e-5 & 3.6\,e-5 & 1.7\,e-5 \\ -1.1\,e-5 & -2.2\,e-5 & -3.2\,e-5 & -1.7\,e-5 & 1.7\,e-5 & 3.6\,e-5 & 5.5\,e-5 & 2.5\,e-5 \\ -5.5\,e-6 & -1.1\,e-5 & -1.7\,e-5 & -2.1\,e-5 & 7.5\,e-6 & 1.7\,e-5 & 2.5\,e-5 & 3.4\,e-5 \end{bmatrix} \begin{bmatrix} -54 \\ -281 \\ -281 \\ -54 \\ 0 \\ 0 \\ 0 \\ 0 \end{bmatrix} = \begin{bmatrix} -0.14\,e-1 \\ -0.28\,e-1 \\ -0.28\,e-1 \\ -0.14\,e-1 \\ 0.1\,e-1 \\ 0.17\,e-1 \\ 0.17\,e-1 \\ 0.1\,e-1 \end{bmatrix} \text{in.} \quad (9.12)$$

Loads to apply to left connections of panel 5:

$$\boldsymbol{F} = \boldsymbol{k_{4x4}X} = \begin{bmatrix} 44193 & -20211 & 12.29 & 63.61 \\ -20211 & 40611 & -20460 & 12.29 \\ 12.29 & -20460 & 40611 & -20211 \\ 63.61 & 12.29 & -20211 & 44193 \end{bmatrix} \begin{bmatrix} 0.1\,e-1 \\ 0.17\,e-1 \\ 0.17\,e-1 \\ 0.1\,e-1 \end{bmatrix} = \begin{bmatrix} 85.5 \\ 144.6 \\ 144.6 \\ 85.5 \end{bmatrix} \text{lb.} \quad (9.13)$$

Deflections of connection locations of panel 5

$$\boldsymbol{X} = \boldsymbol{mF} = \begin{bmatrix} 3.4\,e-5 & 2.5\,e-5 & 1.7\,e-5 & 7.5\,e-6 & -2.1\,e-5 & -1.7\,e-5 & -1.1\,e-5 & -5.5\,e-6 \\ 2.5\,e-5 & 5.5\,e-5 & 3.6\,e-5 & 1.7\,e-5 & -1.7\,e-5 & -3.2\,e-5 & -2.2\,e-5 & -1.1\,e-5 \\ 1.7\,e-5 & 3.6\,e-5 & 5.5\,e-5 & 2.5\,e-5 & -1.1\,e-5 & -2.2\,e-5 & -3.7\,e-5 & -1.7\,e-5 \\ 7.5\,e-6 & 1.7\,e-5 & 2.5\,e-5 & 3.4\,e-5 & -5.5\,e-6 & -1.1\,e-5 & -1.7\,e-5 & -2.1\,e-5 \\ -2.1\,e-5 & -1.7\,e-5 & -1.1\,e-5 & -5.5\,e-6 & 3.4\,e-5 & 2.5\,e-5 & 1.7\,e-5 & 7.5\,e-6 \\ -1.7\,e-5 & -3.2\,e-5 & -2.2\,e-5 & -1.1\,e-5 & 2.5\,e-5 & 5.5\,e-5 & 3.6\,e-5 & 1.7\,e-5 \\ -1.1\,e-5 & -2.2\,e-5 & -3.2\,e-5 & -1.7\,e-5 & 1.7\,e-5 & 3.6\,e-5 & 5.5\,e-5 & 2.5\,e-5 \\ -5.5\,e-6 & -1.1\,e-5 & -1.7\,e-5 & -2.1\,e-5 & 7.5\,e-6 & 1.7\,e-5 & 2.5\,e-5 & 3.4\,e-5 \end{bmatrix} \begin{bmatrix} 85.5 \\ 144.6 \\ 144.6 \\ 85.5 \\ 0 \\ 0 \\ 0 \\ 0 \end{bmatrix} = \begin{bmatrix} 0.1\,e-1 \\ 0.17\,e-1 \\ 0.17\,e-1 \\ 0.1\,e-1 \\ -0.6\,e-2 \\ -0.1\,e-1 \\ -0.1\,e-1 \\ -0.6\,e-2 \end{bmatrix} \text{in.} \quad (9.14)$$

Loads to apply to left connections of panel 6:

$$\boldsymbol{F} = \boldsymbol{k_{4x4}X} = \begin{bmatrix} 44193 & -20211 & 12.29 & 63.61 \\ -20211 & 40611 & -20460 & 12.29 \\ 12.29 & -20460 & 40611 & -20211 \\ 63.61 & 12.29 & -20211 & 44193 \end{bmatrix} \begin{bmatrix} 0.6\,e-2 \\ 0.1\,e-1 \\ 0.1\,e-1 \\ 0.6\,e-1 \end{bmatrix} = \begin{bmatrix} -63.5 \\ -80.3 \\ -80.3 \\ -63.5 \end{bmatrix} \text{lb.} \quad (9.15)$$

The loads from Equation 9.15 show the effect loading panel 1 has on panel 6. Note, this same procedure can be used to find the effect loading panels 2-5 has on panel 6. The point loads required to induce a displacement on panel 6 that matches the effect of loading panels 1-5 can then be superimposed assuming the concentrated load is within the linear range. The final super imposed load on panel 6 from loading panels 1-5 is shown in Equation 9.16. The superimposed loads from loading panels 1-5 shown in Equation 9.16 can then be applied to the left connection locations of panel 6. The transverse and longitudinal 12 psi loads can then be applied to panel 6. The simulation

can then be run, the results interpreted, and the design can be changed accordingly.

$$\boldsymbol{F_{tot}} = \begin{bmatrix} -63.5 \\ -80.3 \\ -80.3 \\ -63.5 \end{bmatrix} + \begin{bmatrix} 85.5 \\ 144.6 \\ 144.6 \\ 85.5 \end{bmatrix} + \begin{bmatrix} -54 \\ -281 \\ -281 \\ -54 \end{bmatrix} + \begin{bmatrix} -20 \\ 523 \\ 523 \\ -20 \end{bmatrix} + \begin{bmatrix} 264.5 \\ -1000 \\ -1000 \\ 264.5 \end{bmatrix} = \begin{bmatrix} 212.6 \\ -693.7 \\ -693.7 \\ 212.6 \end{bmatrix} \text{lb.} \tag{9.16}$$

9.3 Distribution of Loads Using the Compliance and Stiffness Matrices

Figure 9.3 shows that the deflections of a given panel change sign from the left connection point of a panel to the right connection point of a panel for panels 2-6. The panel deflections not only change sign, but they also grow smaller in absolute value the farther the panels are from the loaded panel. One would expect this trend. A heavily loaded panel does not greatly impact a panel that is 10 panels away; however, one would expect that the first few adjacent panels would be affected by the heavy concentrated load. Stanton (1992) uses a triangular distribution width for his analysis on the response of a floor system to a single panel under a heavy concentrated load. The term triangular is used to define how the intensity of a response of a single loaded panel begins with a peak at the location of the load, and then dies off and eventually reaches zero in an affine manner. As Stanton asserts in his reasoning behind the use of a triangular distribution width, "[T]he true distribution is a decaying exponential, which is much more closely simulated by a triangle" (Stanton, 1992).

In order to verify that the method used in this thesis follows the generally accepted distribution shape of various flooring systems, a plot of the absolute value of deflections is shown in Figure 9.4. Note that the exponential trend line almost perfectly matches the data. Figure 9.4 shows that the intensity of the response calculated using the compliance matrix method decays in an exponential manner, as one would expect.

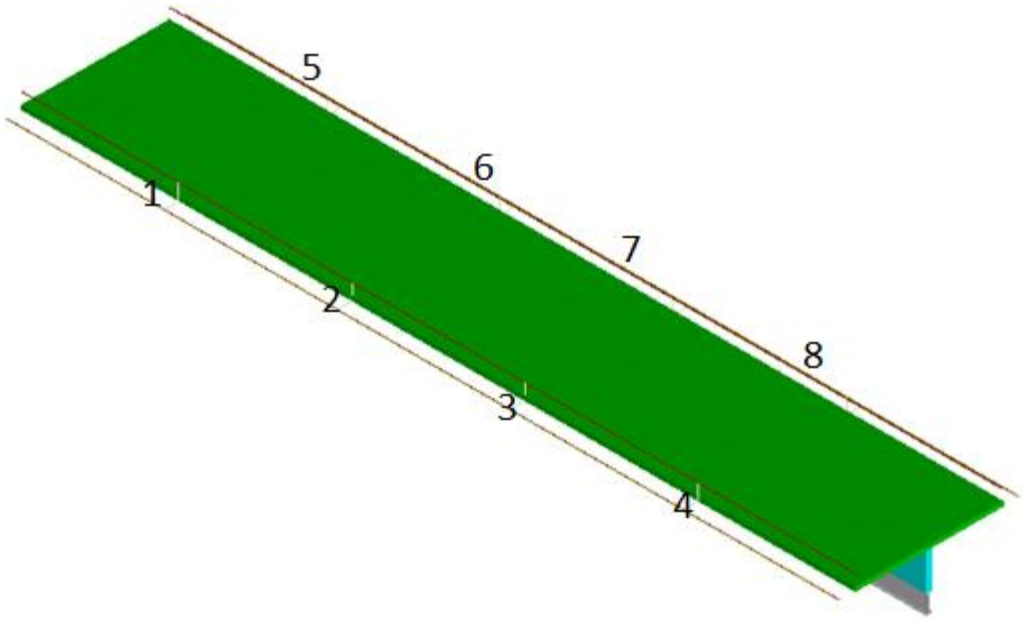

Figure 9.1: Constructed Conditions Panel

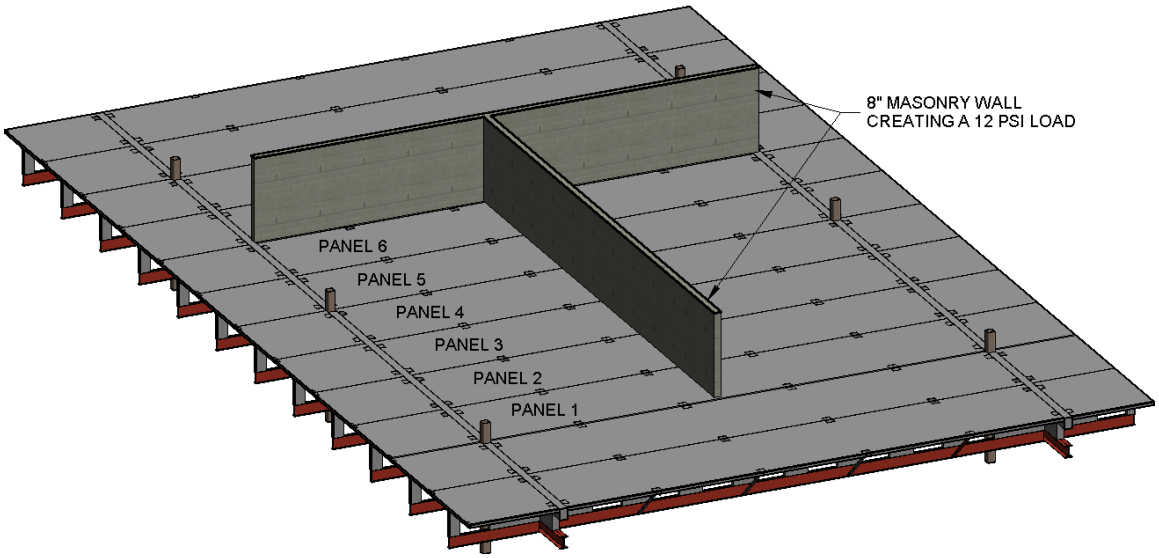

Figure 9.2: Asymmetrical Floor Loading Scenario

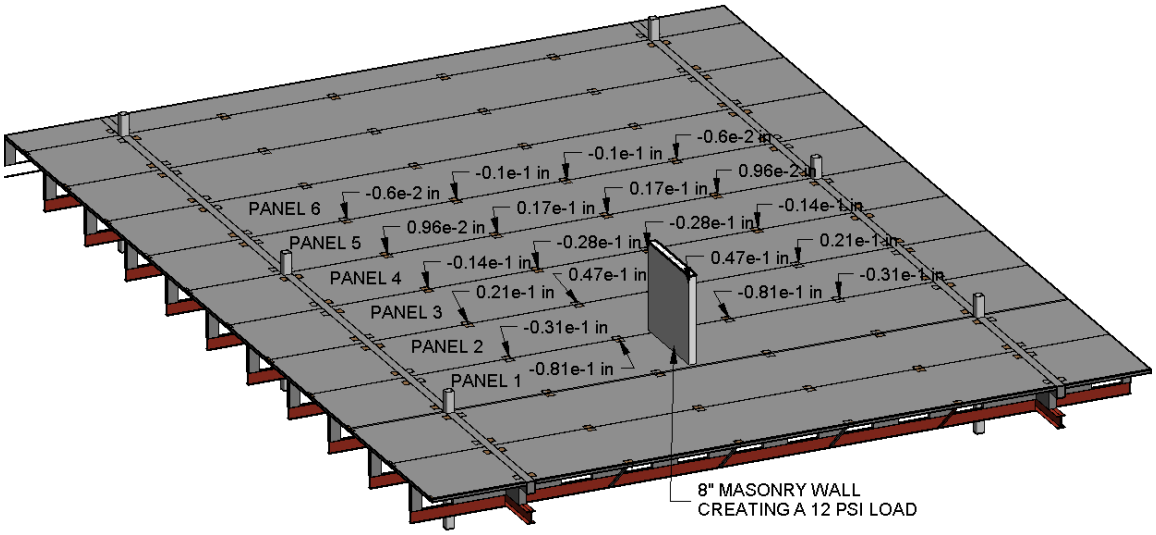

Figure 9.3: Panel Deflections Due to Load on Panel 1

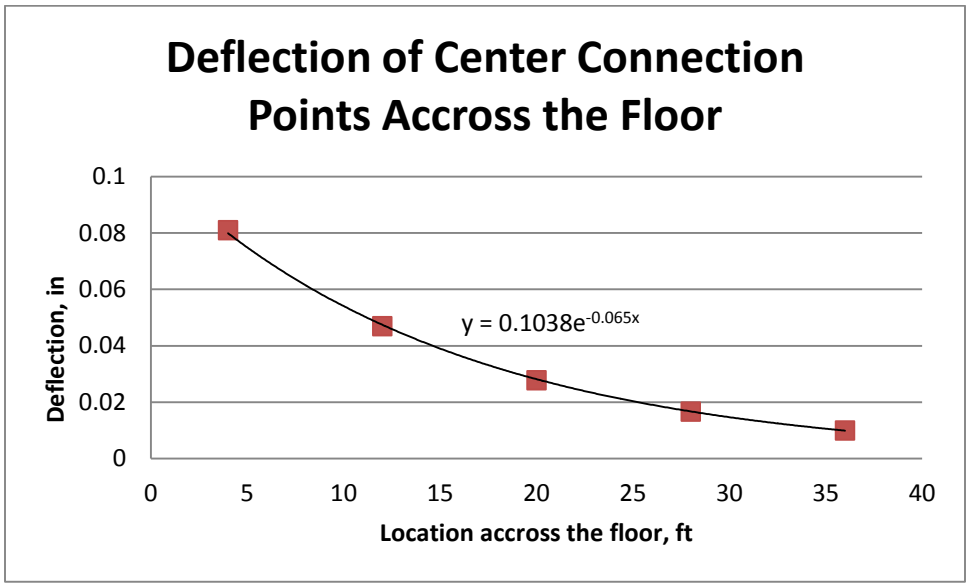

Figure 9.4: Deflection of Panel Connection Points

CHAPTER 10

CONCLUSIONS

This study develops a method to analyze the constructed performance of a precast flooring system using finite element software. The floor system used to develop this method is the Plattforms flooring system. As shown in Chapter 2, this flooring system is comprised of a composite steel beam and concrete slab. The slab is connected to the steel beam through a system of concrete stem walls. As with most precast systems, the general method used to analyze the Plattforms flooring system is applying a uniform load to the entire section, and then using the section properties to calculate the stresses and deflections. The original model used to analyze the system was a simple Euler-Bernoulli beam theory model. In this model, Plattforms, Inc. assumed that strain was linear from tension in the steel to compression in the concrete. Research by Burkhart (2010) at the University of Utah shows that strain is not linear. At failure of the precast member during the tests, the bottom 7.5 in. of the 10 in. steel member was in tension. The top 2.5 in. of the steel went into compression (Burkhart, 2010). To account for the reduced equivalent moment of inertia created by the deformation of the stem walls, Plattforms, Inc. uses a stiffness reduction factor that closely matches test data, but is based on sparse empirical data.

Hollow-core decks, double-T sections, and various other precast flooring systems

are also analyzed using uniform loads. The Plattforms system slightly differs from these other systems in that the Plattform section has concrete blockouts that change the section properties of the member at different locations along the longitudinal axis. Analyzing the Plattforms members as an Euler-Bernoulli beam is not correct analytically, as test data have repeatedly pointed out. Research performed at the University of Utah shows that the strain distribution is not linear through the stem walls, and that some of the steel beam experiences compression. Full-scale tests performed at Mountain States Steel show that the deflections calculated using Euler-Bernoulli theory are inaccurate. Fortunately, software programs such as ANSYS can be used to analyze complex sections. Chapter 7 showed that by applying the appropriate boundary conditions and material properties, ANSYS can accurately model the deflection of the Plattforms system under a uniform load.

In reality, loads are never uniform. There are many occasions that a concentrated load is applied to a panel at some distance from the panel's centerline. Researchers have investigated the effects of heavy concentrated loads on precast panels. The primary purpose of previous research was to investigate how the load on one panel would affect the performance of the adjacent panels. Empirical relationships that help define a "distribution width" for a load have been determined in past research. The distribution width would be used by designers to distribute a heavy concentrated load to adjacent panels.

The work performed in this thesis differs substantially from the work performed by previous researchers The method used to analyze the constructed conditions of a panel in this thesis are described in Chapter 3 and reiterated here for clarity:

1. Perform verification testing of elements that will be used in the finite element model to ensure understanding of the constitutive relationships used by the software;
2. Create a finite element model of a single panel;
3. Compare the results of the finite element model to test results;
4. Modify the model to reflect the constructed conditions by varying the boundary conditions;
5. Create floor plan loading scenarios for the structure to represent a wide range of possible conditions;
6. Apply appropriate loads to the finite element model (these could include vibratory loads); and
7. Interpret results and modify design if necessary.

Step 1 is a commonly overlooked step in finite element analysis; however, one must have an understanding of the constitutive relationships used by the finite element software tool they plan to use for their analysis. Chapter 5 shows some simple single element testing that was used to analyze the constitutive relationships of the elements that were implemented in the three-dimensional model.

In step 2, a three-dimensional model of the panel under analysis is created. For this thesis, the model is a replica of the panels tested in the Mountain States Steel tests. This model uses the same material properties as the materials used in the test. Because the tests performed at Mountain States Steel utilized uniform loads, a ¼ panel model is used, and appropriate boundary conditions are applied to save on computing time.

Step 3 is to compare the results of simulations to the test results. As shown in

Chapter 7, the model created coupled with appropriate boundary conditions accurately reflects the results of the Mountain States Steel tests. The validation of the model through comparison to tested results is a critical step in the process.

Step 4 is to change the boundary conditions to reflect the constructed conditions of the panel. The tests performed at Mountain States Steel do not reflect the constructed conditions expected in a panel. During the tests at Mountain States Steel, there was no torsional restraint at the girder, and the panel-to-panel connections were not used. Chapter 8 shows how the constructed condition boundary conditions are created. The panel-to-panel connections are modeled as a cable substructure. The stiffness of the cable is determined by applying point loads to the edge of panel that is assumed to be connected to girders on three sides. The fourth side is assumed to be free from any restraint. The deflections at the connection locations for every permutation of point loads are then analyzed. The analysis shows that the deflections at the connection locations can be modeled as a cable of a given tension. Once the appropriate tension is found for the panel that is connected to girders on three sides, a substructure of cables is used to model that panel. This substructure is then connected to a panel that is connected to girders on only two sides. The stiffness at the free connection locations (free meaning not connected to a girder or a cable substructure) is then found by applying point loads to the connection locations. This process continues until the tension in the cables does not change as other panels are added to the system.

Step 5 uses the constructed condition model to analyze an asymmetrical floor load on an arbitrary floor plan. A concentrated load applied to a single panel has an effect on adjacent panels. Chapter 9 shows how this effect on adjacent panels can be analyzed

using the constructed conditions model. Using the terminology from Chapter 9, a single loaded constructed conditions panel has deflections at each of the connection locations. The adjacent panel has the same deflections at the connection locations due to the compatibility at the connections. The deflections induced on the adjacent panel by the loaded panel can be re-created on the adjacent panel by applying point loads at the connection locations of the adjacent panel. These point loads can be found through a 4×4 stiffness matrix. The effect of the deflections induced by the loaded panel can be propagated across the floor through the use of an 8×8 compliance matrix in conjunction with the 4×4 stiffness matrix. The effects of all of the loaded panels on the selected panel can then be found by superposition of the point loads required to induce the appropriate deflection on the selected panel.

Steps 6 and 7 in this process are to run the analysis of the selected panel with the floor loads, and the induced point loads from the rest of the loaded panels. Once the simulation has been run in ANSYS, deflections and stresses can be analyzed, and changes in design can be made. More research, however, should be done prior to using this method in practice. Tests should be performed to validate the accuracy of the cable substructure. A single panel could be subjected to point loads at the connection locations. The tested deflections at the connection locations could then be compared to the analytical data. These tests could also show if panels would rub together at the edges under heavy loads. The interface between the panels may play a role in the deflection behavior at the edges of a panel. The edge of a heavily loaded panel may come into contact with the adjacent panel and create deflections in the adjacent panel through means other than just the connections. Friction created between the heavily loaded panel

edge and the adjacent panel may change the behavior of load transfer from the loaded panel to the adjacent panel. Thick topping slabs also play a role in how loads are transferred from the loaded panel to the adjacent panel.

Future modeling should also include the stiffness of the girders. Up to this point, the girders were considered infinitely rigid in comparison to the Plattform panel. In reality, the stiffness of the girder is a function of location on the girder. Near a girder support, the girder can be assumed as infinitely rigid; however, at the midspan of the girder, there may be deflection that could alter results. The stiffness of the girder becomes very important when analyzing the vibration properties of the Plattforms system. Assuming the girders to be infinitely stiff increases the frequency of the fundamental modes of vibration. Typical human traffic occurs at a frequency of 1 to 3 Hz. A stiff structure has fundamental modes of vibration that have substantially higher frequencies than 1 to 3 Hz. Falsely stiffening a structural element may give frequencies that are too high, and may not reflect the actual vibration characteristics of the structural element in a building.

The method shown in this thesis allows researchers to perform in-depth analysis of a single panel in the constructed condition state. Utilizing the simple substructure that models the stiffness of the adjacent floor, the constructed condition performance can be found for any type of gravity load. Asymmetrical loads can be analyzed in a quantitative manner that shows the stress distribution and deflection effects across a floor assembly. Future research is still required, but this technique opens a door which could allow designers to perform in depth analysis of the constructed conditions of any precast flooring system.

REFERENCES

ACI 318. Building Code Requirements for Structural Concrete; American Concrete Institute: Farmington Hills, MI, 2008.

AISC. Steel Construction Manual, 13th Edition; American Institute of Steel Construction: Chicago, IL, 2005.

ANSYS Elements Reference. ANSYS Release 10.0; ANSYS Inc.: Canonsburg, PA, 2005.

Burkhart, B. Behavior and Analysis of Plattforms Building System. Master's Thesis, University of Utah, Salt Lake City, UT, 2010.

Chen, Y. Finite Element Analysis for Walking Vibration Problems for Composite Precast Building Floors Using ADINA: Modeling, Simulation, and Comparison. Computers and Structures 1999, 72, 109-126.

Hawileh, R. A.; Rahman, A.; Tabatabai, H. Nonlinear Finite Element Analysis and Modeling of Precast Hybrid Beam-Column Connection Subjected to Cyclic Loads. Applied Mathematical Modeling 2010, 2562-2583.

Mahmoud, A. M. Strengthening of Concrete Having Shear Zone Openings Using Orthotropic CFRP Modeling. Ain Shams Engineering Journal 2012, 177-190.

PCI Design Handbook. Precast and Prestressed Concrete, 6th Edition; Precast Concrete Institute: Chicago, IL, 2004.

Stanton, J. Response of Hollow-Core Slab Floors to Concentrated Loads. PCI Journal 1992, 98-113.

Western Technologies. Mountain States Steel Test Results; Western Technologies: Phoenix, AZ, 2010